ΕΛΛΗΝΙΚΗ
ΕΠΙΣΤΗΜΟΝΙΚΗ
ΕΤΑΙΡΕΙΑ
ΕΔΑΦΟΜΗΧΑΝΙΚΗΣ
& ΓΕΩΤΕΧΝΙΚΗΣ
ΜΗΧΑΝΙΚΗΣ

Mammoth ferns flourish between the narrow walls of Claustral Canyon in New South Wales, Australia

Τα Νέα της Ε Ε Ε Ε Γ Μ

110

Αρ. 110 – ΙΑΝΟΥΑΡΙΟΣ 2018

SIMSG ISSMGE

ISRM

On behalf of the Hellenic Society of the European Association for Earthquake Engineering and Aristotle University of Thessaloniki, I have the great pleasure to invite you to the 16th European Conference on Earthquake Engineering (16thECEE), to be organized in Thessaloniki, Greece between 18-21, June, 2018.

In the light of the previous successful conferences we have committed ourselves to deliver a well-tailored and focused event of the highest scientific and organizational standards in a vibrant and friendly city renowned for its beauty, its warm hospitality and history, spanning more than 2000 years.

We are sure that you will find participation in 16th ECEE professionally rewarding, scientifically stimulating and personally enjoyable. We look forward to welcoming you to Thessaloniki in June 2018.

Π Ε Ρ Ι Ε Χ Ο Μ Ε Ν Α

Mount Roraima Venezuela cliffs

Paraglide over the Canadian Rockies

Rainbow Bridge, Lake Powell in Utah Arizona

The Colorado River cuts around Grand Canyon National Park

ΑΡΘΡΑ

Το παρακάτω άρθρο, στην συγγραφή του οποίου συμμετέσχε το μέλος της ΕΕΕΕΓΜ Δρ. Κώστας Σαχπάζης, κατετάγη στην δεύτερη θέση των καλύτερων άρθρων που δημοσιεύθηκαν στο περιοδικό The Electronic Journal of Geotechnical Engineering το 2017.

Slope Stability Evaluation for the New Railway Embankment using Stochastic Finite Element and Finite Difference Methods

Eleyas Assefa, Dr. Li Jian Lin, Dr. Costas I. Sachpazis, Dr. Deng Hua Feng, Dr. Sun Xu Shu, Xiaoliang Xu

ABSTRACT Evaluation of Slope stability is one of the day-to-day practices of geotechnical engineers. Nowadays, different methods are available to evaluate the stability of a particular slope. Despite the advances that have been made in site exploration, evaluating the stability of slopes remains a challenge. Recently, Ethiopia has been trying to construct a newly planned railway routes to connect the country's development centers and link with ports of neighboring countries. However, this newly planned railway routes will pass in the heart of highly fragile mountainous terrains and earthquake prone regions. Therefore, the prime objective of this paper is to investigate the stability of the railway embankment by using three different stochastic approaches (First Order Reliability Method, Point Estimate Method and Monte Carlo Simulation) with commercially available finite element and finite difference programs. Moreover, the seismic response of the railway embankment was studied by using a nonlinear analysis (FLAC2D v 7.0) program. The first order reliability method (FORM), Monte Carlo Simulation (MCS) and Point-estimate method (PEM) gave 3.2%, 4.14% and 1.5% of probability of failure respectively. In the mean time, there was no any indication of liquefaction observed due to stiff foundation clay soils and deep groundwater table.

INTRODUCTION

Evaluation of Slope stability is one of the day-to-day practices of geotechnical engineers. Nowadays, different approaches are available to evaluate the stability of a particular slope [1], [2], and [3]. Despite the advances that have been made, evaluating the stability of slopes remains a challenge [4], [5], [6], and [7]. The fundamental requirement for stability of slopes is that the shear strength of the soil must be greater than the shear stress required for equilibrium [1] and [2]. If the shear stress exceeds the shear strength of the soil, different forms of slope failure will occur [8], [9], [10], and [11]. Recently, Ethiopia has been trying to construct a newly planned railway routes to connect the country's development centers and link with ports of neighboring countries. However, this newly planned railway routes will pass in the heart of highly fragile mountainous terrains and earthquake prone regions. Previously, the authors of this paper [12] did a probabilistic slope stability evaluation for the new railway embankment found in Ethiopia, using Quake/w and Slope/w programs. In their study, several different conditions, reflecting different stages in the life of the new railway embankment were simulated. The long term and short term stability of the railway embankment were investigated. The corresponding factors of safety were 2.585 and 2.199 respectively. Moreover, three different approaches were applied to scrutinize the effect of earthquake on the stability of the railway embankment. The pseudo-static analyses were done by using the conventional approach (the corresponding factor of safety was 1.221) and the effective stress approach (the corresponding factor of safety was 1.656). Then Newmark's deformation analysis was carried out [12]. The factor of safety (1.695) was obtained by using the results of Quake/w analysis into slope/w program. Finally, the sensitivity study on the railway embankment revealed that the shear strength parameters of the silt clay foundation soil (layer-II) will govern the stability of the railway embankment. The previous study was based on the limit equilibrium (LE) slope stability analysis. However, it is important to point out that, limit equilibrium methods cannot provide the lower bound. But, sometimes it will furnish lower factor of safety than the one computed by using the finite element (FE) methods [13]. In this case one should not rely up on the LE solution.

Therefore, the prime objective of this paper is to investigate the stability of the previously studied railway embankment [12] by implementing three different stochastic approaches (First Order Reliability Method, Point Estimate Method and Monte Carlo Simulation) into commercially available finite element and finite difference programs. To meet this objective, only pseudo-static analysis was chosen to perform the stochastic analysis, in view of the fact that pseudo-static analysis gave the minimum factor of safety for this particular railway embankment [12]. If the strength of the soil is reduced less than 15 percent by cyclic loading, pseudo-static analyses of the earthquake loading can be used [1]. However, some engineers perform dynamic analysis for all slopes, even if the strength reduction due to earthquake loading is less than 15 percent [1]. Knowing that, dynamic analyses are very complex, involve considerable uncertainties, and are if the strength of the soil is reduced more than 15 percent as a result of cyclic loading, dynamic analyses are needed to estimate the deformations that would result from earthquakes [1]. Despite its simplicity, pseudo-static analyses produced factor of safety above 1 would fail during earthquakes [1], [14], and [15]. This shows the inability of pseudo-static method to reliably evaluate the stability of slopes susceptible to weakening instability (Liquefaction). Regarding to this, there have been tremendous works to evaluate the liquefaction susceptibility of fine grained soils [16], [17], [18], [19], [20], [21], [22], [23], [24], and [25]. Nonetheless, there is no universally acceptable guideline to evaluate the liquefaction potential of fine grained soils. As it was discussed by Prakash [26], "It is obvious that it is still not possible to evaluate the likelihood of liquefaction of silts or silty clays with the same confidence as for clean sands without additional investigations". For this reason, the seismic response of the railway embankment was studied by using a nonlinear analysis (FLAC2D v 7.0). The standard practice for dynamic analysis of earth structures, and especially analyses dealing with liquefaction, is based primarily upon the equivalent-linear method. The nonlinear numerical method has not been applied as often in practical design [13]. However, the equivalent-linear method takes drastic liberties with physics, but is user-friendly and accepts laboratory results from cyclic tests directly [13]. The fully nonlinear method correctly represents the physics, but demands more user involvement and needs a comprehensive stress-strain model in order to reproduce some of the more subtle dynamic phenomena.

METHODS AND MATERIALS

Project Location

Awash – Kombolcha – Hara Gebaya Railway Project is a 390 km long railway (Figure 1a) between cities of Awash (km 0), Kombolcha (~km 270) and Hara Gebaya (~km 390). Currently, this railway project is under ongoing construction. Previously, the authors of this paper [3] suggested the method of analyses to be adopted for the newly planned railway routes in Ethiopia. In this paper, a particular critical high fill railway embankment at Km 261+140 was chosen for the stability analyses. This railway embankment is located in close proximity to Kombolcha city (Ethiopia). Figure 1b shows typical railway embankment fill on the specified site.

Figure 1a: Newly planned railway routes

Figure 1b: Typical railway embankment

Soil Properties

The soil strata at km 261+140 are mainly composed of over-consolidated cohesive soils ranging from stiff to very stiff clay soils. Important geotechnical properties of the railway embankment and the foundation materials are shown in Table 1. After careful extrapolation of the ground water table from the nearby boreholes, the groundwater table was estimated (11m from the ground surface), and the expected surcharge load on the embankment was 15kPa [12].

When the cohesion of embankment soil specified as zero, the minimum factor of safety will always tend towards the infinite slope case. Moreover, the critical slip surface will be parallel and immediately next to the slope face [27]. To overcome such situation and to get a more realistic slip surface, soil suction was considered. For many years the significance of suction has never been quantified [28]. According to Fredulund [28], the suction in an unsaturated soil increases the cohesion of the soil. Accordingly, the shear strength parameters used in a slope stability analysis should be modified to reflect the in-situ soil suction condition. Fredulund [28] suggested that the suction of a soil could be considered as an increase in cohesion. Considering the relationship among pore radius, matric suction, and capillary height, the cohesion of the embankment material was defined to as 5kPa.

Table 1: Geotechnical properties of the railway embankment

Parameters	Fill	Silty clay (layer I)	Silty clay (layer II)	Silty clay (layer III)	Rock
Thickness (m)	14	2	11.5	8.1	8.4
γ uns (kN/m3)	20	18	18	18	20
γ sat (kN/m3)	20	18	18	18	20
E(kPa)	50,000	15,000	17,000	25,000	300,000
υ	0.25	0.35	0.35	0.35	0.25
Cu (kPa)	-	100	100	100	-
C (kPa)	0	20	20	20	20
ϕ	40	26	26	26	42
Vs (m/s)	-	177	303	389	811
G(kPa)	20,000	5,555.6	6,296.3	9,259.3	120,000
K(kPa)	33,333.3	16,666.7	18,888.9	27,777.8	200,000
porosity	0.3	0.3	0.3	0.3	0.3

Shear Strength Reduction Approach

Finite element and finite difference methods have wide application in geotechnical engineering. Specially, with the development of computers these method have been increasingly used and they have been a popular tool to evaluate the stability of slopes [1], [29], and [30]. Some of the advantages of finite element approach over the limit equilibrium methods in the analysis of slope stability problems were given by Griffiths and Lane, 1999 [30]. Unlike limit equilibrium approach, finite element method doesn't require any Prior assumptions about the location, direction and shape of the failure surface [1] and [2]. In the mean time, FEM can accurately determine stress, strains and the corresponding shear strengths. It is a powerful tool to monitor the progressive failure [1]. However, it has also drawbacks relative to the limit equilibrium methods. For instance, lack of complex models and the difficulty of incorporating some features like tension cracks and reinforcement in the stability model [1]. Slope stability evaluation using finite element and finite difference methods can be done by using the strength reduction approach [29], [30], [31], [32], [33], [34], and [35]. In this technique, the shear strength of the material will be artificially reduced till a state of limiting equilibrium achieved. The method is commonly used with Mohr-Coulomb failure criterion. The safety factor F is defined according to the following equations.

$$C^{trial} = \frac{1}{F^{trial}} C \tag{1}$$

$$\phi^{trial} = \tan^{-1}\left(\frac{1}{F^{trial}} \tan\phi\right) \tag{2}$$

Pseudo-static Analysis

As it was mentioned previously, if the strength of the soil is reduced less than 15 percent by cyclic loading, *pseudo-static* analyses of the earthquake loading can be used [1]. In this analysis a unidirectional pseudo-static acceleration was applied through the sliding mass. Considering the previous study [12], a peak ground acceleration of 0.3g for 10% probability of occurrence in 50 years was opted for the analysis. Although engineering judgment is required for all cases, the criteria of Hynes-Griffin and Franklin (1984) should be appropriate for most slopes [1]. Therefore, using the criteria provided by Hynes-Griffin and Franklin (1984) [36]; an acceleration multiplier factor of 0.5 and 80% of the static shear strength were used for the pseudo-static analysis. Moreover, the pseudo-static analysis was done by using effective stress approach (the one suggested by Marcuson (1990)) [37], where excess pore water pressures are used to represent the post-earthquake strengths, effective stress shear strength parameters and excess pore water pressures are used in lieu of undrained shear strengths for the first-stage analysis.

Slope Stability Evaluation using stochastic approach

Uncertainty and risk are central features of geotechnical and geological engineering. Engineers can deal with uncertainty by ignoring it, by being conservative, by using the observational method, or by quantifying it [6]. In recent years, the uses of reliability analysis and probabilistic methods have been increasing in geotechnical engineering and related fields [1] and [6]. In the past, several researchers conducted slope stability analysis by using probabilistic approach [30], [38], [39], [40], [41], [42], [43], and [44].

Central problem facing the geotechnical engineer is to establish the properties of soils and rocks that will be used in the analysis, whether that analysis is probabilistic or deterministic [45]. However, to develop a reliable design approach, one must use statistical methods to deal with the variability of input parameters.

In this study, among the most commonly used methods; First Order Reliability Method (FORM), Monte-Carlo Simulation (MCS) and Point–Estimate Methods (PEMS) were used together with commercially available finite element and finite difference programs, to study the stability of the rail way embankment under pseudo-static analysis. Some of the advantages and disadvantages of these methods have been discussed in detail by Christian and Baecher (2003) [6].

The N-Sigma Rule

In this particular site, fissures or cracks were observed in the clay deposits. Some of the fissures were several meters in length and depth, especially in areas with deep groundwater table. Therefore, both sample recovery and strength testing were very difficult on these fissured clays. In this situation, testing of an intact sample may give an unrealistically high strength, and fissured sample unrealistically low strength. Therefore, considerable engineering judgment was required to derive the design parameters. Similarly, in geotechnical engineering the values of soil properties are frequently estimated based on correlations or on meager data plus judgment [1], [46], and [47], and it is not possible to use the standard deviation equation to determine the standard deviation. However, the N-Sigma rule (Foye 2006) [48] provides a means of taking into account the fact that an engineer's experience and available information. N-Sigma rule is expressed as follows:

$$N_\sigma = \frac{H_{cv} - L_{cv}}{N_\sigma} \quad (3)$$

where: H_{cv} and L_{cv} are the highest and lowest conceivable values of the parameter respectively. According to [1] a better estimate of standard deviation would be made by dividing the range by 4. This conclusion (i.e., N_σ=4) was made based on the works of Christian and Baecher (2001) [49].

As it was mentioned in the introduction part, the sensitivity study [12] on the railway embankment revealed that the shear strength parameters of the silty-clay foundation soil (layer-II) will govern the stability of the railway embankment. Therefore, the shear strength parameters of the foundation soil (layer II) were considered as random variables. Based on Hynes-Griffin and Franklin (1984) criteria, 80% of the static shear strength parameters were determined, and these values were defined as the most likely values for the pseudo-static analysis. Then N-sigma rule was used to compute the standard deviations of the random variables (4kPa for the cohesion and 4.26 degree for the internal angle of friction) as shown in Table 2.

Table 2: Determination of standard deviation for foundation soil (layer II) based on the N_σ rule

Silty-clay foundation soil (layer II)	L_{CV}	H_{CV}	M_{LV}*	σ	COV
Cohesion (kPa)	8	24	20*0.8=16	4	0.25
Angle of friction (degree)	12.8	29.85	$\tan^{-1}$(0.8* tan26)= 21.31	4.26	0.2

*most likely value (M_{LV})

Furthermore, the computed coefficients of variations (COV) in Table 2 have been compared with the existing literatures [6] and [50], and they were found in a good agreement with the published data. Both cohesion and internal angle of friction were assumed as statistically independent parameters. As it is well known, many natural data sets follow a bell-shaped distribution and measurements of many random variables appear to come from population frequency distributions that are closely approximated by a normal probability density function. This is also true for many geotechnical engineering material properties. Figure 2a and 2b represented the assumed probability density function for the random variables.

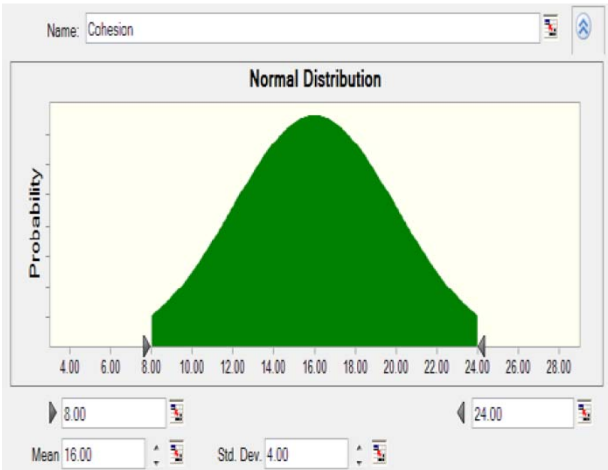

Figure 2a: PDF for cohesion

First Order reliability Method

First Order Reliability Method (FORM) is the simplest and the most widely used method, started by assuming that all the (x_i-μ_{xi}) terms are small, so their squares, cubes, and higher powers will be even smaller, and can be ignored [51]. Since only the first order terms are included, methods based on this assumption are called First Order Reliability Method (FORM).

In this paper, the algorithm, suggested by Rackwitz and Fiessler (1978) [51] was adopted to conduct the pseudo-static slope stability analysis for the railway embankment.

This method linearizes the performance function at each iteration point; and uses the derivatives to find the next iteration point. Compared to other nonlinear optimization algorithms available in the literature, the algorithm just described requires the least computation at each step. The next iteration point is computed using a single recursive formula that requires information only about the value and the gradient of the performance function. The storage requirement is therefore minimal. The algorithm is also found to converge fast in many cases [51]. The procedures used in this method are described herein under.

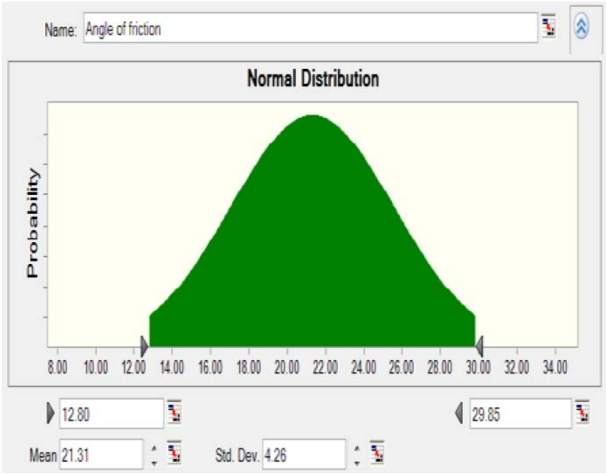

Figure2b: PDF for internal angle of friction

Step 1: Define the appropriate performance function.

Step 2: Assume initial values of the design point: x_i^*, i=1, 2,…, n, and compute the corresponding value of the performance function *g( )*. In the absence of any other information, the initial design point can be the mean values of the random variables.

Step 3: Compute the mean and standard deviation at the design point of the equivalent normal distribution for those variables that are not normal.

$$x_i'^* = \frac{x'_{i} - \mu^N_{X_i}}{\sigma^N_{X_i}} \quad (4)$$

Step 4: Compute the partial derivatives $\partial g/\partial x_i$ evaluated at the design point x_i^*.

Step 5: Compute the partial derivatives $\partial g/\partial x_i'$ in the equivalent standard normal space.

Step 6: Compute the partial derivatives $\partial g/\partial x_i'$ in the equivalent standard normal space.

$$\frac{\partial g}{\partial X_i'} = \frac{\partial g}{\partial X_i}\sigma^N_{X_i} \quad (5)$$

The components of the corresponding unit vector are the direction cosines of the performance function, computed as

$$\alpha_i = \frac{\left(\frac{\partial g}{\partial x_i}\right)^* \sigma^N_{X_i}}{\sqrt{\sum_{i=1}^{n}\left(\frac{\partial g}{\partial x_i}\sigma^N_{X_i}\right)^{2*}}} \quad (6)$$

Step 7: Compute the new values for the design point in the equivalent standard normal space (x'^*_i) using the following recursive formula:

$$x'^*_{k+1} = \frac{1}{|\nabla g(x'^*_k)|^2}[\nabla g(x'^*_k)^t - g(x'^*_k)]\nabla(x'^*_k) \quad (7)$$

Where: $\nabla g(x_k'^*)$ is the gradient vector of the performance function, at $x_k'^*$, iteration point. Note that k refers to the iteration number. Therefore $x_k'^*$ is a vector with components $[x_{1k'}^*, x_{2k'}^*, \ldots, x_{nk'}^*]^t$, where n is the number of random variables.

Step 7: Compute the distance (β) to this new design point from the origin.

$$\beta = \sqrt{\sum_{i=1}^{n}(x_i'^*)^2} \quad (8)$$

Check the convergence criterion for β (Δβ≤0.005).

Step 8: Compute the new values for the design point in the original space (x_i^*) as

$$x_i^* = \mu^N_{X_i} + \sigma^N_{X_i} x_i'^* \quad (9)$$

And compute the value of the performance function g () for the new design point, check g () is very close to zero within 0.005. If both convergence criterions satisfied stop the computation, otherwise, repeat Steps 3 through 8 until convergence. To evaluate the partial derivatives of the performance function, central finite difference method was used as:

$$\left(\frac{\partial g}{\partial c}\right)^* = \frac{f(c^*+\Delta c, \emptyset^*) - f(c^*-\Delta c, \emptyset^*)}{2\Delta c} \quad (10)$$

Where: c^* and $\emptyset^*$ are values of shear strength parameters at the design point. Here, Δc was defined as 10percent of the standard deviation of cohesion (i.e., Δc=0.1*4=0.4). The factor of safety of the railway embankment was evaluated at ($c^*+\Delta c, \emptyset^*$) and ($c^*-\Delta c, \emptyset^*$). Then the partial derivatives of the performance function were easily determined.

$$\left(\frac{\partial g}{\partial \emptyset}\right)^* = \frac{f(c^*, \emptyset^*+\Delta\emptyset) - f(c, \emptyset^*-\Delta\emptyset)}{2\Delta\emptyset} \quad (11)$$

Where: ΔØ was defined as 10percent of the standard deviation of internal angle of friction (i.e., ΔØ =0.1*4.26=0.426)

Monte Carlo simulation Using FLAC 2D v7.0

In contrast to the traditional limit equilibrium codes, FLAC provides a full solution of the coupled stress/ displacement, equilibrium and constitutive equations. In FLAC the failure surface is delineated by the concentration of shear strain contours. In this study, a fine-grid model was used, since it can clearly define the shear strain contours. Then, the pseudo-static slope stability analysis was done by implementing a Monte Carlo simulation into FLAC.

The Monte Carlo Simulation (MCS) is a powerful and popular tool for the evaluation of uncertainties in engineering practices [52] and [53]. It can be applied for both correlated and un-correlated random variables [54]. However, the number of simulations can affect the accuracy of the technique. In this paper, Box and Muller [55] algorithm was used to generate a pair of random deviates from the same normal distribution starting from a pair of random numbers.

Let *U1, U2* be independent random variables from the same rectangular density function on the interval (0, 1). Consider the random variables:

$$x_1 = (-2\log_e U_1)^{1/2} \cos(2\pi U_2) \quad (12)$$

$$x_2 = (-2\log_e U_1)^{1/2} \sin(2\pi U_2) \quad (13)$$

$$x_i = \mu_x + N_i\sigma_x \quad (14)$$

Then (x_1, x_2) will be a pair of independent random variables from the same normal distribution with mean zero, and unit variance. The normal variables were determined by using the mean and standard deviation.

A FISH program was written to generate probabilistic input variables and their random combinations were used to perform a number of deterministic computations. Outliers of shear strength parameters have been excluded during the analysis. Beside, a mean factor of safety for the railway embankment was determined by using the mean shear strength parameters. The failure criterion was defined in terms of nodal unbalanced force ratio. If the unbalanced force ratio is less than 10-3 after N steps, then the system is in equilibrium [13]. However, if the unbalanced force is greater than 10-3, then it will be considered as a failure. The following flowchart (Figure 3) clearly demonstrates the procedures used in the analysis.

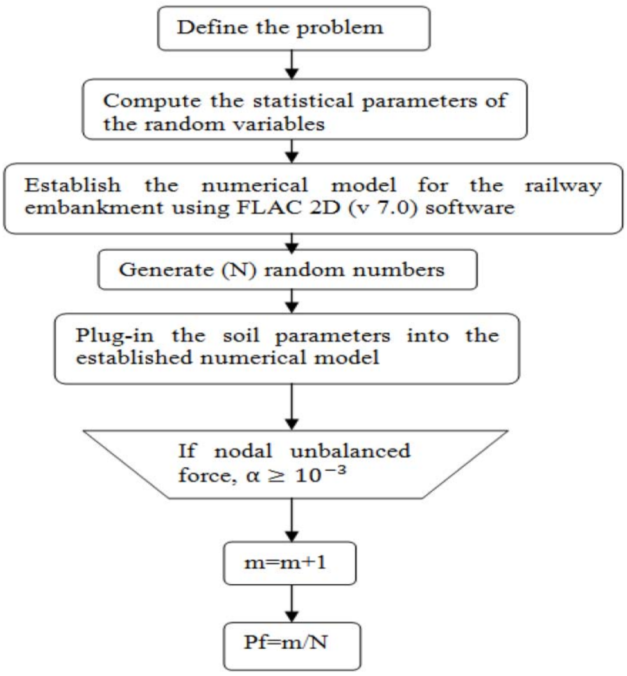

Figure 3: Flow chart for Monte Carlo Simulation used in FLAC2D program

The probability of failure for the railway embankment was computed by using the ratio of the total number of failures to the total number of Monte Carlo simulations. Finally, the standard deviation of safety factors was determined by using the Z-table together with Equation (15).

$$Z = (x-\mu) / \sigma \quad (15)$$

Where x is the variable of interest μ is the mean, and σ is the standard deviation.

Reliability index (β) was determined by using the following equation.

$$\beta = (\mu-1) / \sigma \quad (16)$$

Point Estimate Method using Phase² v8.0

The point estimate method was performed, by using the commercially available finite element program (Phase² v8.0). This program has been used in the design and analysis of mining, tunneling and surface excavations. However, few applications have been reported in the area of slope stability analysis [56]. The slope stability analysis for the railway embankment was done by using the strength reduction factor (SRF) approach. Phase² v8.0 enables the user to carry out a probabilistic slope stability analysis based on the Rosenblueth two-point-estimate method, for the first and the second moment of uncorrelated variables. Though the two-point-estimate method is easy to use and satisfactorily accurate for a range of practical problems, it has also some detriments [6]. The main limitation of this method is that, it deals with normal distribution only. The other constraint is, even if all the inputs follow normal distributions the outputs may not be normally distributed and the point estimate method approximation can be inaccurate. Figure 4 shows the stepwise procedures used during the analysis. The factors of safety were evaluated by using four different combinations (Figure 4).

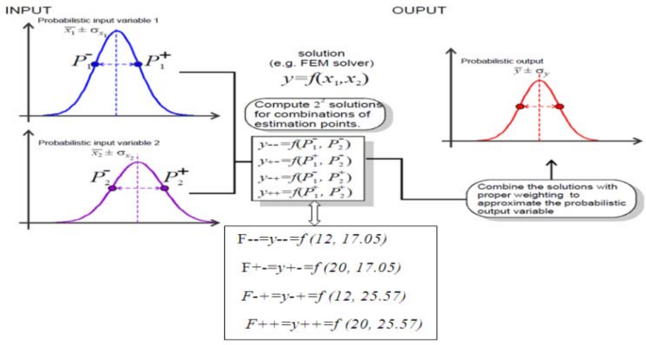

Figure 4: Computation principle of two point estimate method used in Phase² v 8.0

Dynamic Analysis of the railway embankment

Estimation of Representative Material Properties

In this analysis, the foundation and embankment soils were modeled as elastic-perfectly plastic Mohr-Coulomb materials. The geotechnical properties of the railway embankment are listed in Table 1. Average relationships between the dynamic shear moduli and damping ratios of soils, as functions of shear strain and static properties, have been published for various soil types [57]. Therefore, the dynamic characteristics of all of the soils in this model were assumed to be governed by the modulus reduction factor (G/Gmax) and damping ratio (λ) curves, as shown in Figure 5.

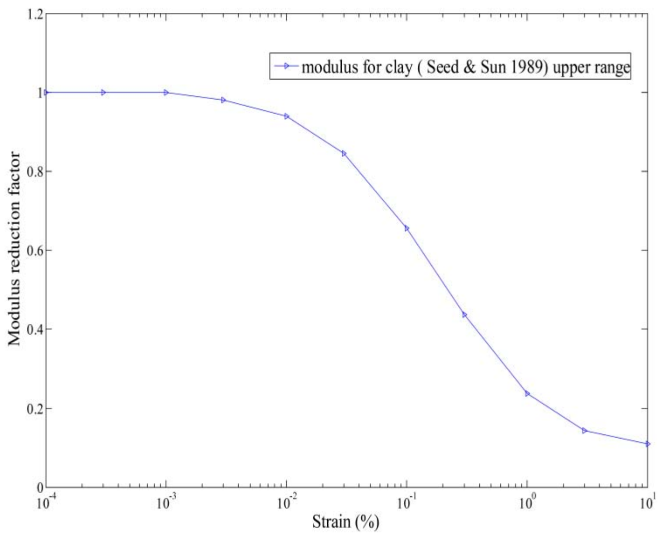

(a) Modulus reduction curve for Clay

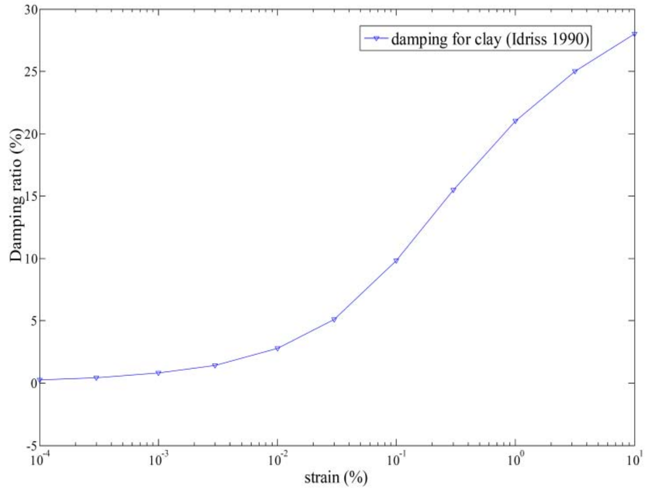

(b) Damping ratio curve for Clay

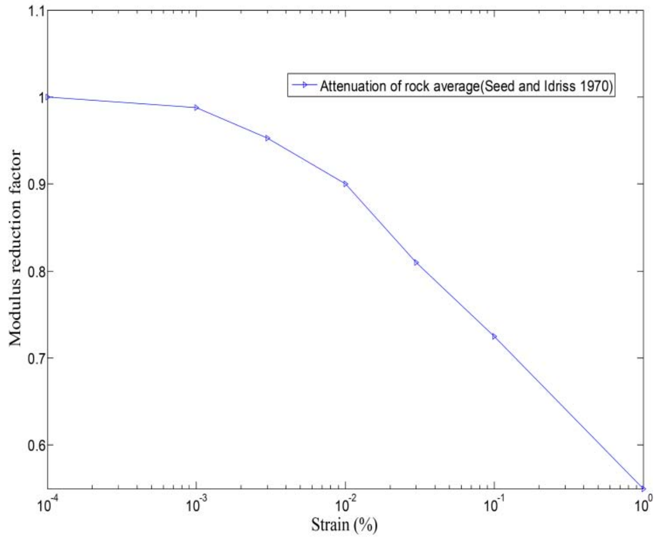

(c) Modulus reduction curve for Rock

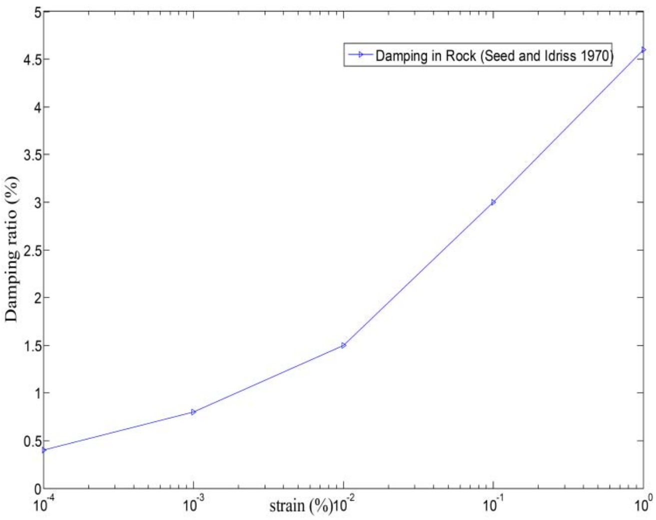

(d) Damping ratio curve for Rock

Figure 5: Dynamic characteristics of the soil/ Rock used in Shake2000 model Rayleigh Damping Parameters

The equivalent linear program SHAKE2000 was run to estimate the Rayleigh damping parameters to represent the inelastic cyclic behavior of the soils in the FLAC model, based upon the curves in Figure 5. A SHAKE2000 free-field column model was created for the foundation soils as shown in Figure 6. The second and the third layers in the free-field column were subdivided into 5 and 3 equal sub layers (Table 3). Similarly, the rock layer was subdivided into two sub layers.

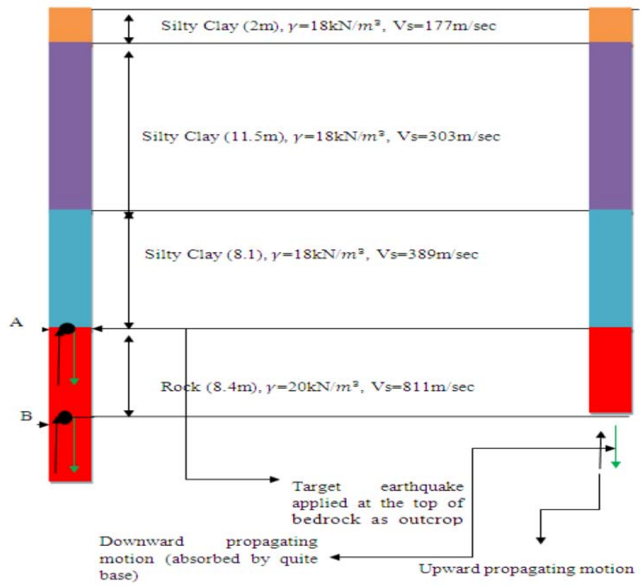

Figure 6: Compliant base deconvolution procedure

The SHAKE2000 analysis was performed using the shear wave speeds, densities, and modulus-reduction and damping-ratio curves for the foundation soils, and the target earthquake motion (The 1940 El Centro (California) earthquake acceleration time history was scaled to the peak ground acceleration of 0.3g to represent the study area) specified for the site. A nominal material damping of 0.1% was used for all layers in order to minimize approximations introduced by the Rayleigh damping model employed in the FLAC analysis (Rayleigh damping is frequency dependent).

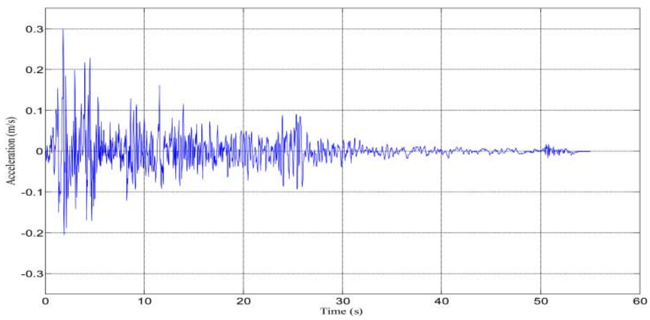

Figure 7: Target earthquake motion applied at the top of bedrock (M=6.7)

Strain-compatible values for the shear-modulus reduction factors and damping ratios throughout the soil column were determined from the analysis. Average modulus-reduction factors and damping ratios were then estimated for the foundations soils based upon the values calculated by SHAKE-2000 and the results are listed in Table 3.

Table 3: Strain compatible damping and modulus reduction for the foundation soil (Shake2000 results)

Thickness (m)	Uniform strain (%)	New Damping	G/Gmax
2.0	0.01918	0.042	0.885
2.3	0.01997	0.042	0.882

2.3	0.03578	0.058	0.819
2.3	0.05183	0.072	0.760
2.3	0.06531	0.081	0.724
2.3	0.07460	0.087	0.703
2.7	0.04140	0.064	0.796
2.7	0.04208	0.064	0.793
2.7	0.04482	0.067	0.783
4.2	0.00854	0.015	0.907
4.2	0.00878	0.015	0.906

Damping ratio and modulus-reduction parameters were selected corresponding to the equivalent uniform strain (which is taken as 50% of the maximum strain) for each layer [13]. The maximum equivalent uniform strain for the foundation soils was defined as 0.075%, the weighted damping ratio and weighted modulus reduction factor were determined as follows:

Weighted damping ratio = 0.051

Weighted G/Gmax = 0.82

The above computed values (damping ratio and modulus-reduction factor) were used as an input for the Rayleigh damping runs in the established FLAC model.

Water Bulk Modulus

In a coupled flow problem, the true diffusivity is controlled by the stiffness ratio R_k (i.e., the stiffness of the fluid versus the stiffness of the matrix):

$$R_k = (k_w / n) / (k + 4G/3) \qquad (17)$$

Where: k_w is the water bulk modulus, n is the porosity, and k and G are the bulk and shear moduli of soil.

The water bulk modulus can be reduced such that R_k = 20 without affecting the results significantly (and reducing the simulation time). Considering the minimum value of shear moduli for layer I, the value of k_w has been adjusted as shown below.

$$R_k = 144444.8\text{kPa}$$

Liquefaction Properties

The liquefaction condition was estimated for the foundation soil (layer II) in terms of standard penetration test results. Average standard penetration number (12.5) for layer II was taken as a normalized standard penetration test value, (N1)60. For a normalized SPT blow count of 12.5, the Finn-Byrne model parameters were C_1 = 0.371 and C_2 = 1.078. Figure 8 shows the borehole log at chainage 261+130.

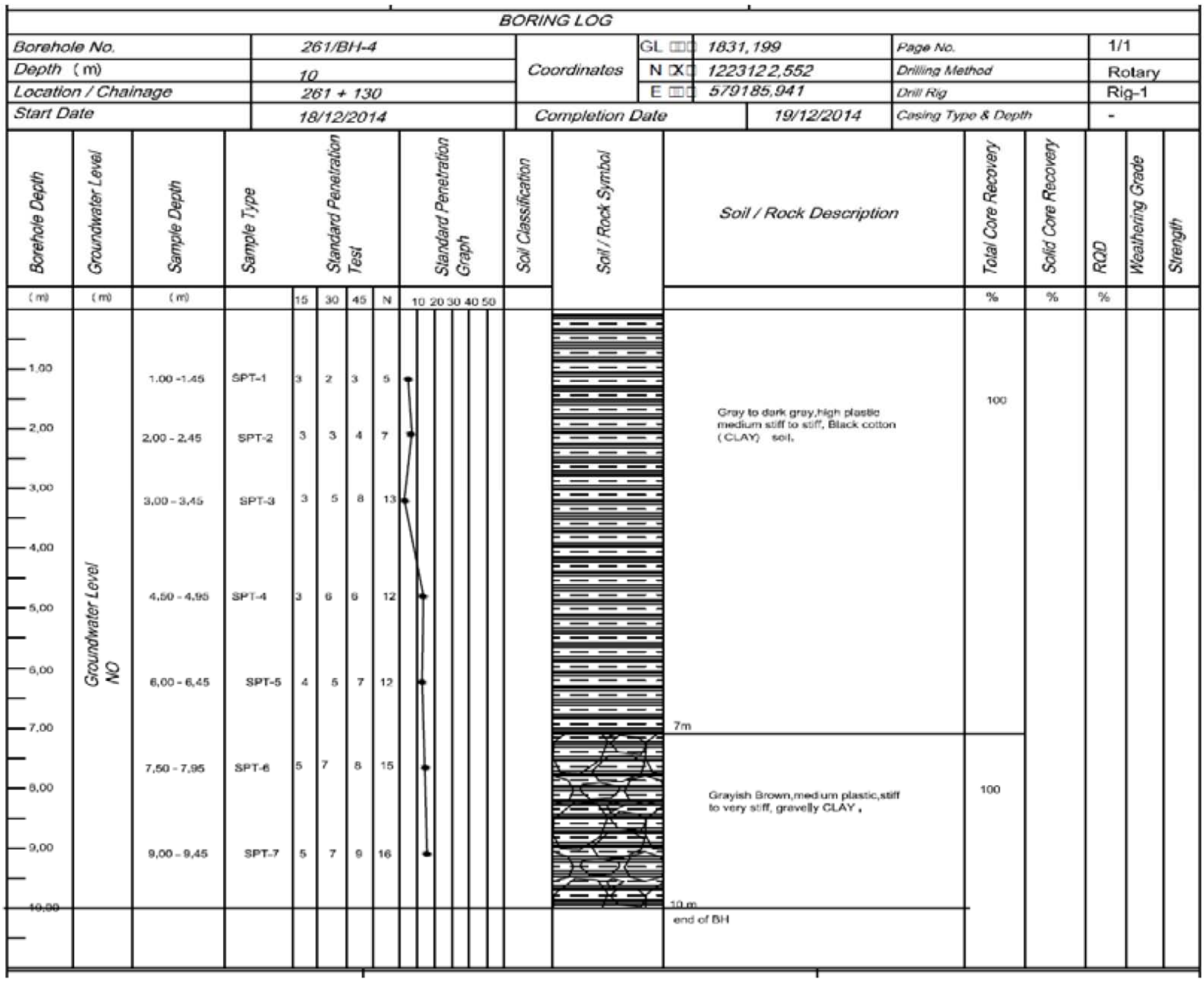

Figure 8: Borehole log at chainage 261+130

Deconvolution Analysis and Estimation of Seismic Motion Characteristics

The deconvolution procedure used in this paper is presented in Figure 6. For the compliant base case there is actually no need to include the soil layers in the SHAKE model as these will have no effect on the upward propagating wave train between points A and B [58]. In this particular case, it is not really necessary to perform a formal deconvolution analysis. This is because the upward propagating motion at point B will be almost identical to that at point A. Apart from an offset in time; the only differences will be due to material damping between the two points, which will generally be small for bedrock [58]. Thus, for this very common situation, the correct input motion for FLAC is simply ½ of the target motion (Figure 9).

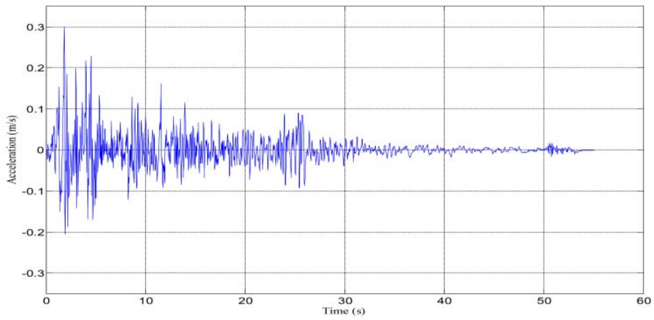

Figure 7: Target earthquake motion applied at the top of bedrock (M=6.7)

Strain-compatible values for the shear-modulus reduction factors and damping ratios throughout the soil column were determined from the analysis. Average modulus-reduction factors and damping ratios were then estimated for the foundations soils based upon the values calculated by SHAKE-2000 and the results are listed in Table 3.

Table 3: Strain compatible damping and modulus reduction for the foundation soil (Shake2000 results)

Thickness (m)	Uniform strain (%)	New Damping	G/Gmax
2.0	0.01918	0.042	0.885
2.3	0.01997	0.042	0.882
2.3	0.03578	0.058	0.819
2.3	0.05183	0.072	0.760
2.3	0.06531	0.081	0.724
2.3	0.07460	0.087	0.703
2.7	0.04140	0.064	0.796
2.7	0.04208	0.064	0.793
2.7	0.04482	0.067	0.783
4.2	0.00854	0.015	0.907
4.2	0.00878	0.015	0.906

Damping ratio and modulus-reduction parameters were selected corresponding to the equivalent uniform strain (which is taken as 50% of the maximum strain) for each layer [13]. The maximum equivalent uniform strain for the foundation soils was defined as 0.075%, the weighted damping ratio and weighted modulus reduction factor were determined as follows:

Weighted damping ratio = = 0.051

Weighted G/Gmax = 0.82

The above computed values (damping ratio and modulus-reduction factor) were used as an input for the Rayleigh damping runs in the established FLAC model.

Water Bulk Modulus

In a coupled flow problem, the true diffusivity is controlled by the stiffness ratio R_k (i.e., the stiffness of the fluid versus the stiffness of the matrix):

$$R_k = (k_w / n) / (k + 4G/3) \qquad (17)$$

Where: k_w is the water bulk modulus, n is the porosity, and k and G are the bulk and shear moduli of soil.

The water bulk modulus can be reduced such that R_k = 20 without affecting the results significantly (and reducing the simulation time). Considering the minimum value of shear moduli for layer I, the value of k_w has been adjusted as shown below.

$$k_w = 144444.8\text{kPa}$$

Liquefaction Properties

The liquefaction condition was estimated for the foundation soil (layer II) in terms of standard penetration test results. Average standard penetration number (12.5) for layer II was taken as a normalized standard penetration test value, (N1)60. For a normalized SPT blow count of 12.5, the Finn-Byrne model parameters were C_1 = 0.371 and C_2 = 1.078. Figure 8 shows the borehole log at chainage 261+130.

Deconvolution Analysis and Estimation of Seismic Motion Characteristics

The deconvolution procedure used in this paper is presented in Figure 6. For the compliant base case there is actually no need to include the soil layers in the SHAKE model as these will have no effect on the upward propagating wave train between points A and B [58]. In this particular case, it is not really necessary to perform a formal deconvolution analysis. This is because the upward propagating motion at point B will be almost identical to that at point A. Apart from an offset in time; the only differences will be due to material damping between the two points, which will generally be small for bedrock [58]. Thus, for this very common situation, the correct input motion for FLAC is simply ½ of the target motion (Figure 9).

A fast Fourier transform (FFT) analysis of the input acceleration record results in a power spectrum as shown in Figure 10. As it can be seen (Figure 10) ,the dominant frequency was approximately 1Hz, the highest frequency component was less than 10 Hz, and the majority of the frequencies are roughly less than 5 Hz. Then the input acceleration was filtered to remove frequencies above 5 Hz (by using the FISH function "FILTER.FIS"). In the mean time, the input record was also checked for baseline drift. The FISH function "INT.FIS" was used to integrate the velocity record again to produce the displacement waveform related to the input acceleration. Then, a baseline correction was performed by adding a low frequency sine wave to the velocity record. And noisy data from the input acceleration were trimmed off at 50 second.

Adjust Input Motion and Mesh Size for Accurate Wave Propagation

The mesh size for the FLAC model was selected to ensure accurate wave transmission. Based upon the elastic properties listed in Table 1, embankment soil layer I has the lowest shear wave speed (177 m/sec). The model used in the analysis has 60 by 19 quadrilateral-zone meshes as shown in Figure 12. The largest zone size in the FLAC model was found to be 2.4m. Then the maximum frequency that can be modeled accurately was:

$$f = (Cs / 10\Delta L) \approx 7.4\text{Hz} \qquad (18)$$

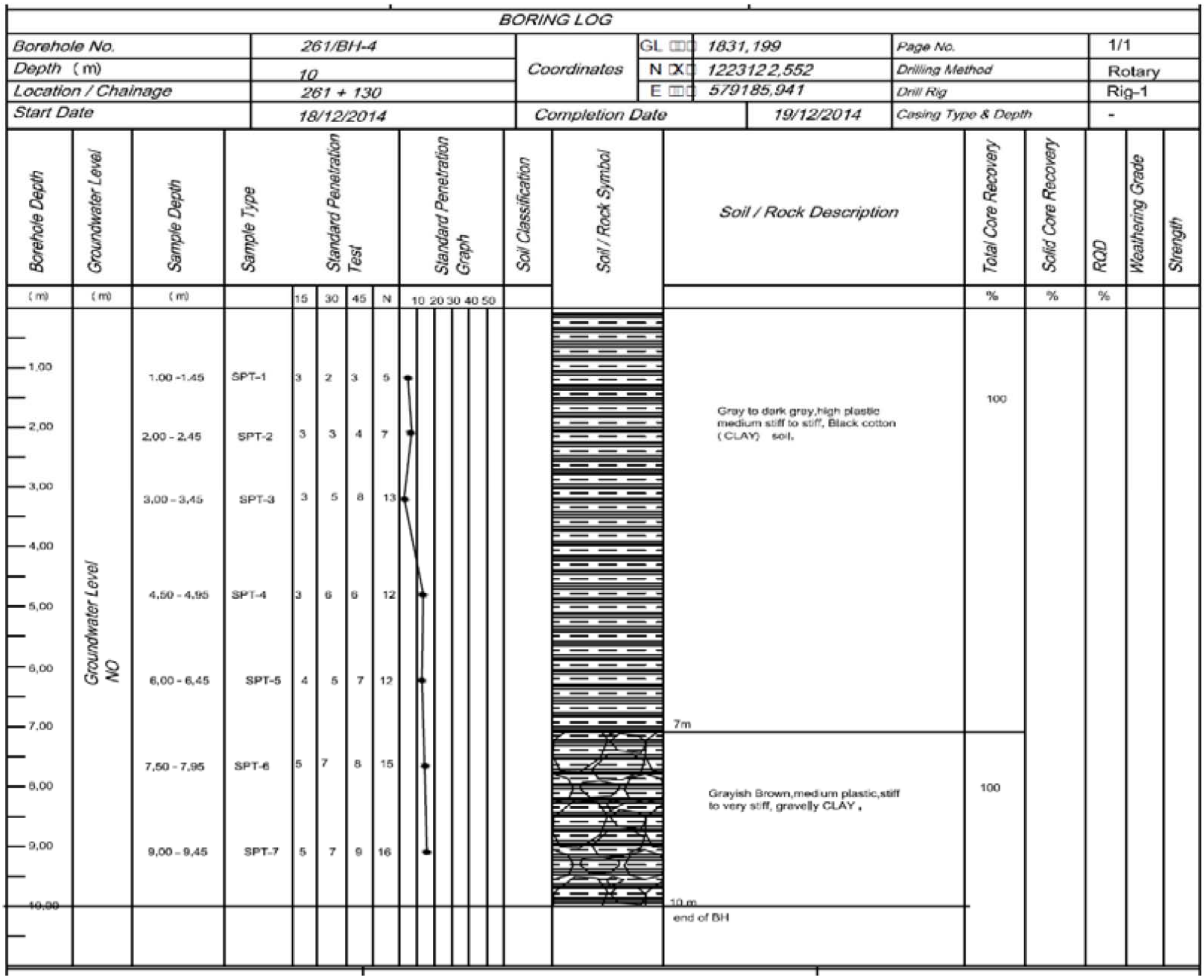

Figure 8: Borehole log at chainage 261+130

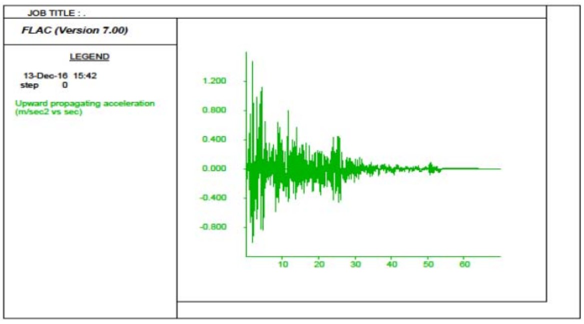

Figure 9: Upward propagating motion (1/2 of the target motion)

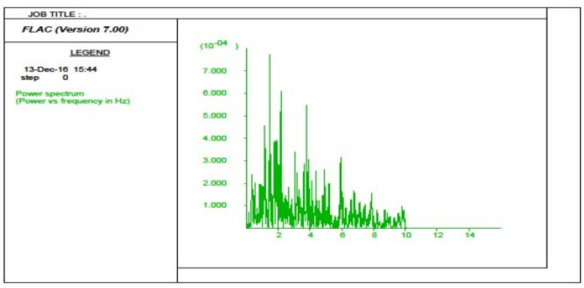

Figure 10: Power spectrum of upward propagating motion (acceleration time history)

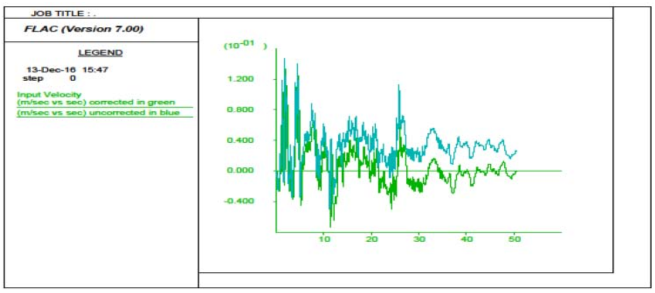

Figure 11: Input velocity used in FLAC with 5Hz filter and baseline correction

As it was previously mentioned, before applying the acceleration input record, it was filtered to remove frequencies above 5 Hz.

Initial state of stress

The analysis was started from the state before the embankment is constructed. Roller boundaries are assigned along the sides of the model, and a fixed boundary along the base was assigned. A fish function ininv was employed to compute the pore pressures and stresses automatically for a model containing a phreatic surface. The function requires the phreatic surface height (wth = 19 for this railway embankment) and the ratios of horizontal to vertical effective stresses (assumed to be k_{0x} = k_{0z} = 0.5). The pore pressure, total stress and effective stress distributions were then calculated automatically. The equilibrium state was checked (using the SOLVE elastic option in the Run/Solve tool).

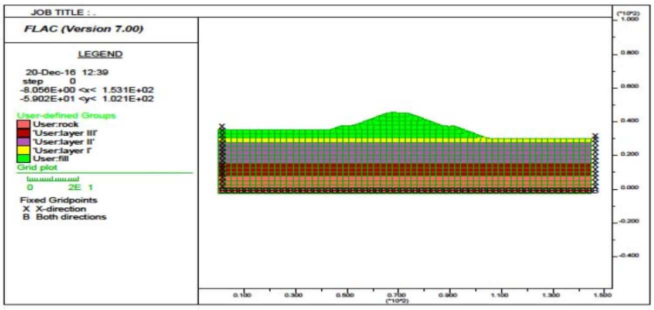

Figure 12: Railway embankment model with foundation and embankment soils assigned

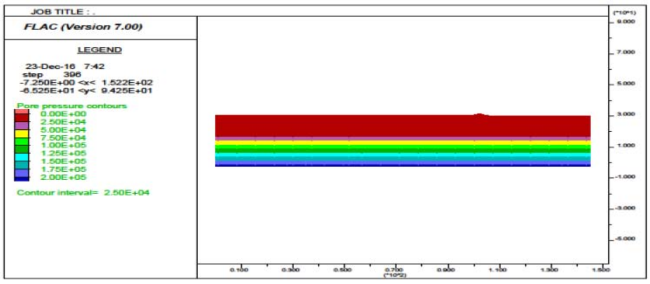

Figure 13: Pore pressure distribution in foundation soils

In this particular railway embankment, the generation of excess pore-pressures and the associated possible liquefaction were not a critical issue at this site, due to the clay foundation and deep groundwater table. Therefore, the embankment was placed in one stage. In addition to the embankment, a surcharge load of 15kPa was introduced into the FLAC model, and the model was run in small-strain mode. This state was considered to be state of the embankment dam at the time of the earthquake event. Then the factor of safety of the railway embankment at this stage was computed.

Dynamic Loading Conditions

For the dynamic loading stage, pore pressures can change in the materials due to dynamic volume changes induced by the seismic excitation. The filtered and baseline-corrected input velocity was called into the established FLAC model. The free-field boundary was set for the side boundaries and a compliant boundary condition was assumed for the base. The dynamic wave was applied as a shear-stress boundary condition along the base after specifying the density, shear wave velocity of the base material and multiplying it by the provided input velocity.

Simulation with Rayleigh Damping

The parameters for the Rayleigh damping model were chosen based on the SHAKE2000 analysis, as it was previously discussed. The initial shear modulus was reduced by a factor of 0.82, and the damping ratio of 0.051was used. The center frequency for Rayleigh damping was 1.0 Hz, as determined from the input wave. The FISH function "GREDUCE.FIS" was executed to reduce the elastic moduli by 0.82 factor.

Seismic Calculation Assuming Liquefaction

Liquefaction is one of important, interesting, complex, and controversial topics in geotechnical earthquake engineering [14]. Fine grained soils (silts and clays) are vulnerable to liquefaction under certain circumstances [26]. There have been a significant controversy and confusion regarding to the liquefaction potential of fine grained soils, as it was pointed out by Seed [20]. Similarly, Prakash [26] signified the deficiency of universally acceptable guidelines to evaluate the liquefaction susceptibility of fine grained soils.

In this analysis, the foundation soil (layer II) was changed to liquefiable material. The Finn-Byrne liquefaction model was prescribed for the foundation soil (layer II), the parameters used for this model was described previously. Cyclic pore-pressure ratio (u_e /σ'_c), was used to identify the likelihood of liquefaction on the foundation soil. Where u_e is the excess pore-pressure and $\sigma'c$ is the initial effective confining stress. Note that a liquefaction state is reached when u_e / $\sigma'_c = 1$.

RESULTS AND DISCUSSIONS

Figure 14 clearly shows the maximum shear strain contours for the railway embankment, using the mean shear strength parameters and pseudo-static analysis. At this stage the mean factor of safety was determined as 1.24. According to Hynes-Griffin and Franklin (1984) [1] criteria the minimum factor of safety for ~1m tolerable displacement is 1.0. Therefore, the mean factor of safety of the railway embankment complied with the specified criteria.

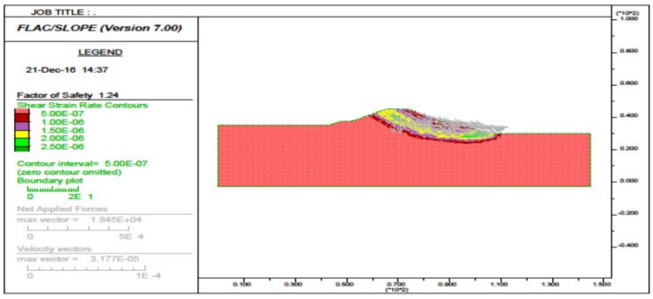

Figure 14: Maximum shear strain contours (Pseudo-static mean factor of safety)

Moreover, similarities in the failure surfaces between FLAC (Figure 14) and slope/w (Figure 15) programs have been observed.

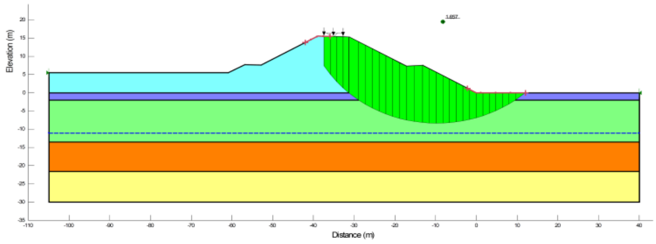

Figure 15: Pseudo-static analysis using effective stress approach and Slope/w [12]

In concept, any slope with a factor of safety above 1.0 should be stable. However, in practice the level of stability is seldom considered acceptable unless the factor of safety is significantly greater than 1.0. This is just to compensate the combined effects of uncertainties in the parameters involved in the slope stability analysis. The reliability of a slope is an alternative measure of stability that considers explicitly the uncertainties involved in the stability analysis. Reliability analysis is an important tool for quantifying uncertainties in geotechnical engineering. Factor of safety and reliability are complement to each other. In this paper, the reliability or probability of failure of a railway embankment was evaluated by using three different stochastic approaches. The results of each method are discussed and presented separately.

Probability of failure using FORM

In this pseudo-static analysis, the random variables (shear strength parameters) were considered as normally distributed and statistically independent parameters. The performance function was defined as *g()=F-1=0*. Where: F is a factor of safety. The stability analysis was done by using FLAC2D program. Each run was done by increasing and reducing the variables by 10 percent of the standard deviation of the corresponding variables. Then central finite difference method was used to evaluate the partial derivatives of the performance function at the design point. The results of this method are tabulated in Table 4. The reliability index (β) for the railway embankment was found to be 1.85 (Table 4). The mean factor of safety (1.24) was determined deterministically by using the mean shear strength parameters of the railway embankment. Then the respective standard deviation was determined after employing Equation 16 as follows:

$1.85 = (1.24-1) / \sigma$, solving for the unknown parameter yielded, $\sigma=0.1297$.

Then Equation 15 was used to get the z value as shown below,

$z = (1-1.24) / 0.1297 = -1.85$

Hence, the probability of failure (3.2%) was determined by using the above result (z=-1.85) together with the Z-Table.

Table 4: Steps used in FORM

Step 1	Defined performance function g()=F-1=0, where F is factor of safety.				
Step 2	Initial values : $c^*=16$, $\emptyset^*=21.3$, and g()=0.24				
Step 3	$\mu^N c$	16	16	16	16
	$\sigma^N c$	4	4	4	4
	$\mu^N \emptyset$	21.3	21.3	21.3	21.3
	$\sigma^N \emptyset$	4.26	4.26	4.26	4.26
	c'^*	0	-0.706	-0.5216	-0.5838
	$\emptyset'^*$	0	-2.824	-1.9210	-1.7560
Step 4	$\left(\frac{\partial g}{\partial c}\right)^*$	0.005	0.0146	0.01463	0.015
	$\left(\frac{\partial g}{\partial \emptyset}\right)^*$	0.0188	0.0505	0.04132	0.03
Step 5	$\left(\frac{\partial g}{\partial c'}\right)^*$	0.02	0.0584	0.05852	0.06
	$\left(\frac{\partial g}{\partial \emptyset'}\right)^*$	0.080	0.2151	0.17602	0.1278
Step 6	New C'^*	-0.706	-0.5216	-0.5838	-0.7868
	New $\emptyset'^*$	-2.824	-1.9210	-1.7560	-1.6759
Step 7	New β	2.910	1.99	1.851	1.851
	$\Delta\beta$		0.92	0.139	0.000
Step 8	New c^*	13.176	13.914	13.665	12.853
	New $\emptyset^*$	9.269	13.117	13.819	14.161
	New g()	-0.205	-0.0254	0.00195	0.00195

Probability of failure using Monte Carlo simulation

The Monte Carlo simulation (MCS) is considered as a very powerful tool for the design and analysis of engineering schemes. In this method, samples of probabilistic input variables were generated and their random combinations were used to perform a number of deterministic computations. However, the accuracy of MCS depends on the number of simulations used in the analysis. To capture this phenomenon, a numerical experiment was conducted. The result showed that, the probability of failure was almost steady while the number of simulations exceeded 1000 (Figure 16a). Therefore in this study, the probability of failure was determined by using 5000 MCS, and it was found to be 4.14%. Then the standard deviation (0.1384) was computed by using Equation 15 and Z-table together. Moreover, the reliability index (β) was evaluated by using Equation 16 as shown below.

$\beta = (\mu-1) / \sigma = 1.73$

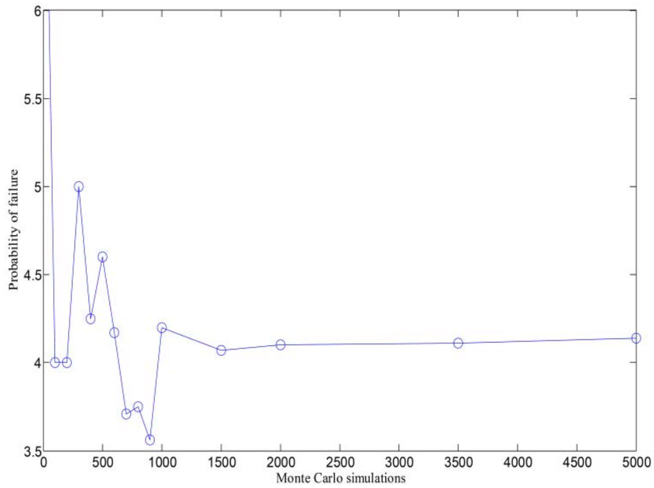

Figure 16a: MCS vs. Probability of failure

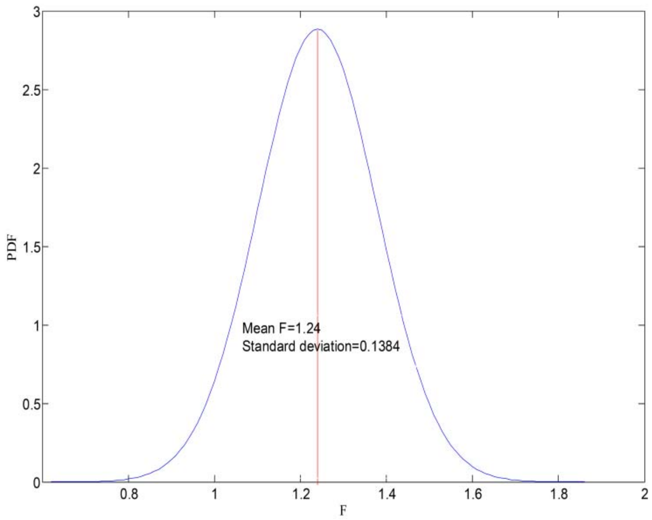

Figure 16b: Normal distribution of F

Since the variability of the soil properties is normally distributed, the probability density function of the factor of safety is also expected to be normally distributed. Therefore, the probability distribution was plotted with MATLAB as shown in Figure 16b.

MCS doesn't require the knowledge of optimization skills, as required by the first-order reliability methods (FORM); and it is mostly general and robust to the dimension of random variables and problem complexity. Nowadays, with the development of powerful personal computers its problem related to time can be minimized.

Probability of failure using Point Estimate Method

Finite element analysis are often computing time intensive and are not well-suited for the multiple runs needed for systematic sensitivity analyses or statistical simulations (eg. Monte Carlo). However, Point estimate method (PEM) is straightforward, easy to use, and requires little knowledge of probability theory. Therefore, the pseudo-static analysis for the railway embankment was carried out by using a built-in simple computing efficient probabilistic method in phase2 finite element program. Based on the results of the analysis (Figure 17), the probability of failure was found to be 1.5%. Similarly, the mean factor of safety and the standard deviation were 1.16 and 0.0714 respectively.

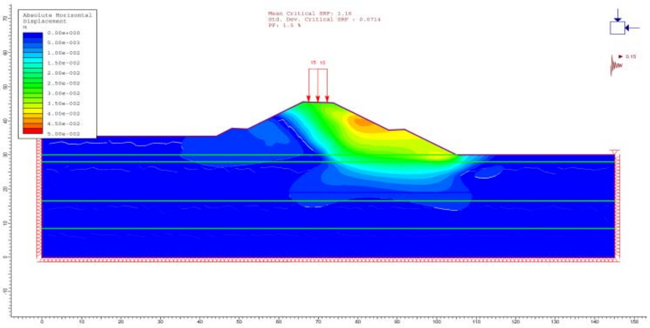

Figure 17: Absolute horizontal displacement using Phase^2 v8.0

While the point-estimate method is popular in practice, it has many detractors. A great limitation of the point-estimate method for multiple variables is that it requires calculations at 2*n* points. When *n* is greater than 5 or 6, the number of evaluations becomes too large for practical applications, even in the day of cheap computer time. The other limitation is, even if all the inputs follow normal distributions the outputs may not be normally distributed and the PEM can be inaccurate [6]. This occurs especially when different behaviors are occurring (e.g. elasticity and plasticity). Besides, the very simplicity of the method suggests to some that the answer is overly approximate. It is worth noting that, two points may not be adequate to obtain accurate estimates of the moments for the function Y in a particular case [6]. Despite these limitations, the method remains a simple, direct, and effective method of computing the low-order moments of functions of random variables.

Dynamic analysis using FLAC

Before evaluating the seismic response of the railway embankment, a factor-of-safety calculation was done as a check on the stability condition at this state (Figure 18). This is considered to be the state of the railway embankment at the time of the earthquake event (F=2.01).

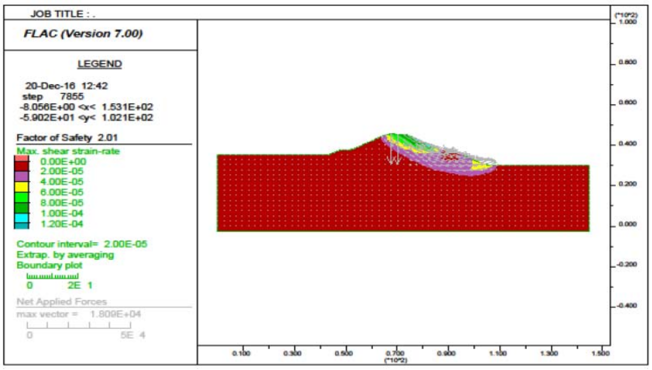

Figure 18: Factor-of-safety plot for railway embankment before earthquake occurred

The maximum shear strain contours throughout the model are plotted for Mohr-Coulomb material and Rayleigh damping and Byrne material and Rayleigh damping in Figure 19 and Figure 20 respectively. Movement of the railway embankment after 50 seconds is primarily concentrated along the left and right side of the slope face. This is clearly shown in the shear-strain increment contour plot.

As it can be seen from Figure 20, the Finn-Byrne model produced noticeable deformations along the lateral (free-field) boundaries of the model. Actually in Dynamic Analysis, the free field boundary performs a small-strain calculation even though the main grid is executing in large strain mode. In order to reduce the mismatch between large-strain and small-strain calculations, the lateral boundaries could be moved farther out. However, this will increase the simulation time.

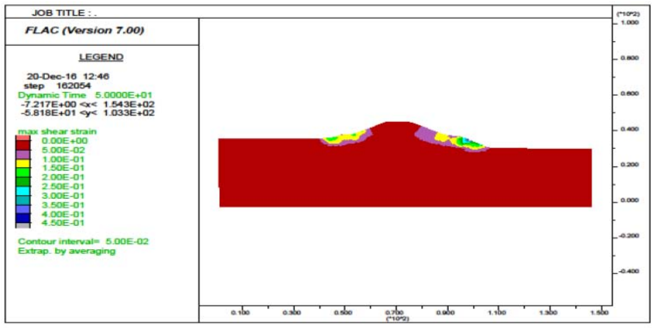

Figure 19: Shear-strain increment contours at 50 seconds–Mohr-Coulomb material and Rayleigh damping

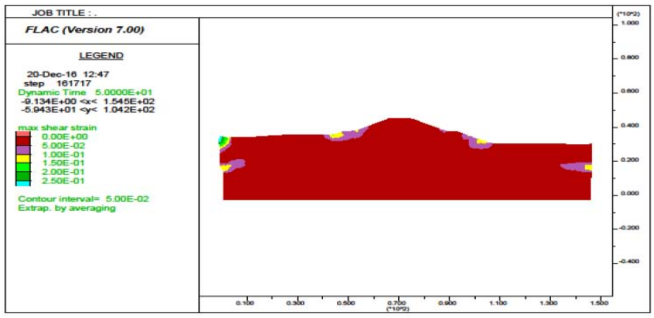

Figure 20: Shear-strain increment contours at 50 seconds – Byrne (liquefaction) material and Rayleigh damping Liquefaction

Figure 21 shows the pore pressure/effective stress measurement at grid point (23, 9), which is nearly at the middle of layer II. Increase in pore pressure (and decrease in effective stress) was observed at this point.

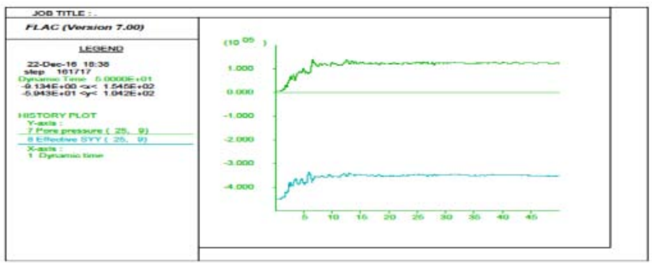

Figure 21: Pore-pressure and effective vertical stress near the middle of layer II – Byrne (liquefaction) material and Rayleigh damping

The normalized excess pore-pressure ratio (or cyclic pore-pressure ratio), u_e/σ_c, can be used to identify the region of liquefaction in the model, where u_e is the excess pore pressure and σc is the initial effective confining stress. A liquefaction state is assumed to occur when u_e/σ_c = 1. The excess pore-pressure ratio was calculated in *FISH* function "GETEXCESSPP.FIS," and the maximum value was stored in *FISH* extra array ex 6. However, for this railway embankment there was no any indication for liquefaction (Figure 22). This is attributed to stiff clay foundation soils and deep ground water table. Liquefaction occurs only in saturated soils, so the depth to groundwater (either free or perched) influences liquefaction susceptibility. Liquefaction susceptibility decreases with the increasing ground water depth [14]. At sites where groundwater levels fluctuate significantly, liquefaction hazards may also fluctuates.

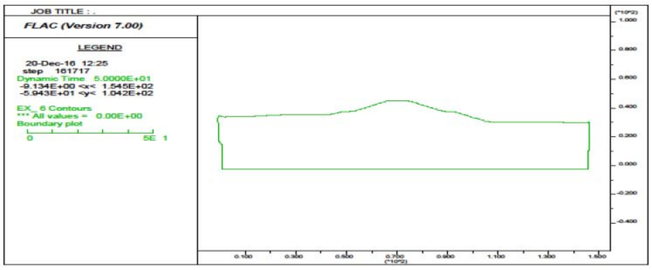

Figure 22: Excess pore-pressure ratio contours (values greater than 0.99) –Byrne (liquefaction) material and Rayleigh damping

CONCLUSIONS

In the preceding pages an attempt has been made to evaluate the slope stability of the new railway embankment found in Ethiopia; using three different stochastic approach together with commercially available finite element and finite difference programs. The main purpose of using reliability models is its capability for becoming an effective mechanism in decision-making process. Probabilistic assessment is more efficient than deterministic methods which are solely relied on the safety factor. The first order reliability method (FORM), Monte Carlo Simulation (MCS) and Point-estimate method (PEM) gave 3.2%, 4.14% and 1.5% of probability of failure respectively. In the mean time, there was no any indication of liquefaction observed due to stiff foundation clay soils and deep groundwater table. For this railway embankment, *pseudo-static* analyses of the earthquake loading can be used, since there is no considerable strength loss by the cyclic loading. Knowing that, dynamic analyses are very complex, involve considerable uncertainties.

ACKNOWLEDGMENT

This research was supported by the National Natural Science Foundation of China (Grant Nos 51309141 and 51479102) and Public welfare Industry Special Fund of Ministry of Water Resources for Scientific Research Projects of China (Grant No. 201401029). The authors would like to acknowledge Engineer Abdulkerim Mohammed, Abdullah Kılıc, Bahadır Sonmez, Dr. Kıvanc Oklap and Suha Abik for their indispensable cooperation.

REFERENCES

1. J. Michael Duncan and Stephen G. Wright (2005). "Soil Strength and Slope Stability". John Wiley & Sons Inc, pp. 293.

2. Abramson, L.W., Lee, T.S., Sharma, S., and Boyce, G.M. (2002). "Slope Stability and Stabilization Methods". John Wiley & Sons Inc, pp.712.

3. Eleyas Assefa, Dr. Li Jian Lin, Dr. Costas I. Sachpazis, Dr. Deng Hua Feng, Dr. Sun Xu Shu, and Dr. Anthimos Anastasiadis (2016). "Discussion on the Analysis, Prevention and Mitigation Measures of Slope Instability Problems: A case of Ethiopian Railways". Electronic Journal of Geotechnical Engineering, vol. 21.12, pp 4101-4119.

4. Phoon, K. K. and F. H. Kulhawy (1999). "Characterization of Geotechnical Variability". Canadian Geotechnical Journal 36: 612-624.

5. Babu, G. L. S., A. Srivastava, et al. (2007). "Analysis of Stability of Earthen Dams in Kachchh Region, Gujarat, India". Engineering Geology 94: 123-136.

6. Gregory B. Baecher and John T. Christian (2003). "Reliability and Statistics in Geotechnical Engineering". John Wiley & Sons Inc, pp. 569.

7. Elkateb, T., R. Chalatumyk, et al. (2003). "An Overview of Soil Heterogeneity: Quantification and Implications on Geotechnical Field Problems." Canadian Geotechnical Journal 40: 1-15.

8. Nemčok, A., Pašek, J. and Rybář, J. (1972). "Classification of landslides and other mass movements" Rock Mechanics, 4: 71-78.

9. Varnes, D. J. (1978). "Slope movements: types and processes. In: Schuster, R.L. and Krizek, R.J. (eds.) Landslide analysis and control". National Academy of Sciences, Transportation Research Board Special Report 176, Washington, 11-33.

10. Hutchinson, J. N. (1988). "General report: Morphological and geotechnical parameters of landslides in relation to geology and hydrology". In: Proc. 5th International Symposium on Landslides, Lausanne, 1: 3-35.

11. Cruden, D. M. and Varnes, D. J. (1996). "Landslide types and processes. In: Turner, A.K. and Schuster, R.L. (eds.) Landslides, Investigation and Mitigation". Transportation Research Board Special Report 247, Washington D.C., 36-75.

12. Eleyas Assefa, Dr. Li Jian Lin, Dr. Costas I. Sachpazis, Dr. Deng Hua Feng, Dr. Sun Xu Shu, and Dr. Anthimos S. Anastasiadis (2016). "Probabilistic Slope Stability Evaluation for the New Railway Embankment in Ethiopia". Electronic Journal of Geotechnical Engineering, vol. 21.11, pp 4247-4272.

13. FLAC and ICG Inc. (2011). "FLAC: Fast Lagrangian Analysis of Continua User's Guide". Itasca Consulting Group Inc., Minneapolis.

14. Kramer, S.L. (1996). "Geotechnical Earthquake Engineering". Prentice Hall, pp. 437.

15. Robert W. Day (2002). "Geotechnical Earthquake Engineering Handbook". McGraw-HILL, pp. 572.

16. Seed H.B., Tokimatsu, K., L.F., and Chung, R. (1985). "Influence of SPT Procedures in Soil Liquefaction Resistance Evaluations". J. Geotechnical Eng'g, ASCE, 111(12), 861- 878.

17. Zhu, S.G. (1981). "Influence of Fines on Evaluating Liquefaction of Sand by CPT". Proc. Int. Conf. on Recent Advances in Geotechnical Eng'g, St. Louis, Missouri, 1: 167-172.

18. Zhou, S.G. (1987). "Soil Liquefaction during Recent Major Earthquakes in China and Seismic Design Method Related to Soil Liquefaction". Proc. 8th Asian Regional Conference on SM&FE, Vol. II, pp. 249-250.

19. Ishihara, K. (1993). "Liquefaction of natural deposits during earthquakes". Proc. 11th ICSMFE, San Francisco, 1, 321-376 Vol. 2, pp. 683-692.

20. Seed, R.B., Cetin, K.O., Moss, R.E.S., Kammerer, A. M., Wu, J., Pestana, J.M. and Riemer M.F. (2001). "Recent Advances in Soil Liquefaction Engineering and Seismic Site Response Evaluation", Proc. 4th Int. Conf. on Recent Adv. in Geotech. Earth. Eng'g and Soil Dynamics, San Diego.

21. Finn, W. D.L., Ledbetter, R. H., R.L. Fleming, R.L., Jr., Templeton, A.E., Forrest, T.W., and Stacy, S.T. (1994). "Dam on Liquefiable Foundation: Safety Assessment

and Remediation" Proc. 17th International Congress on Large Dams, Vienna, pp. 531-553.

22. Bray, Jonathan D., Sancio, R.B., Reimer, M.F. and Durgunoglu, T. (2004). "Liquefaction Susceptibility of Fine grained Soils". Proc. 11th Int. Conf. On Soil Dynamics and earthquake Engineering and 3rd Inter. Conf. on Earthquake Geotech. Eng'g, Berkeley, CA, Jan. 7-9, Vol. 1, pp. 655-662.

23. Boulanger, Ross W. and Idriss, I.M. (2005), "New Criteria for distinguishing Between Silts and Clays That Are Susceptible to Liquefaction versus Cyclic failure". 25th. Annual USSD Conference, Salt Lake City, Utah, June 6-10, pp 357-366.

24. Idriss, I.M. and Boulanger, R.W. (2008). "Soil Liquefaction during Earthquakes", EERI, MNO-12.

25. Towhata, I. (2008), "Geotechnical Earthquake Engineering". Springer Series in Geomehanics and Geoengineering.

26. Shamsher Prakash and Vijay K. Puri (2010). "Recent Advances in Liquefaction of Fine Grained Soils". Fifth International Conference on Recent Advances in Geotechnical Earthquake Engineering and Soil Dynamics, Paper No. 4.17a, pp. 6.

27. GEO-SLOPE International Ltd. (2008). "Stability Modeling with SLOPE/W 2007 Version an Engineering Methodology". GEO-SLOPE International Ltd, Fourth Edition, pp. 347.

28. D.G. Fredulund and H. Rahardjo (1993). "Soil Mechanics for Unsaturated Soils". John Wiley & Sons Inc, pp. 490.

29. Matsui, T., San, K. C. (1992). "Finite element slope stability analysis by shear strength reduction technique". Journal of Soils and Foundation, 32: 59-70.

30. Griffiths, D. V., and Lane, P. A. (1999). "Slope stability analysis by finite elements". Geotechnique 49(3), 387–403.

31. Zienkiewicz, O. C., C. Humpheson, et al. (1975). "Associated and non-associated Viscoplasticity and plasticity in soil mechanics." Geotechnique 25: 671-689.

32. Naylor, D. J. (1981). "Finite elements and slope stability. Numerical methods in Geomechanics". Proceedings of the NATO Advanced Study Institute, Lisbon, Portugal

33. Donald, I. B. and S. K. Giam (1988). "Application of the nodal displacement method to slope stability analysis". Proceedings of the 5th Australia-New Zealand Conference on Geomechanics, Sydney, Australia

34. Dawson, E. M., Roth, W. H., Drescher, A. (1999). "Slope stability analysis by strength reduction". Geotechnique, 49(6): 835-840.

35. Dawson, E. M. and W. H. Roth (1999). "Slope stability analysis with FLAC." Flac and Numerical Modeling in Geomechanics: 3-9.

36. Hynes-Griffin, M. E., and Franklin, A. G. (1984). "Rationalizing the seismic coefficient method". Final Report, Miscellaneous Paper GL-84-13, Department of the Army, U.S. Army Corps of Engineers, Waterways Experiment Station, Vicksburg, MS.

37. Marcuson, W. F., Hynes, M. E., and Franklin, A. G. (1990). "Evaluation and use of residual strength in seismic safety analysis of embankments". Earthquake Spectra, Earthquake Engineering Research Institute, 6(3), 529–572.

38. Matsuo, M., Kuroda, K. (1974). "Probabilistic approach to design of embankments". Soils and Foundations, 14(2): 1-17.

39. Alonso, E. E. (1976). "Risk analysis of slopes and its application to slopes in Canadian sensitive clays". Geotechnique, 26(3): 453-472.

40. Chowdhury, R. N. (1984). "Recent developments in landslide studies: probabilistic methods [A]". In proceedings of the 4th International Symposium on Landslides [C], Toronto, Ont., September 16-21. Canadian Geotechnical Society, 1: 209-228.

41. Wolff, T. F. (1985). "Analysis and design of embankment dam slopes: a probabilistic approach". Ph.D. thesis, Purdue University.

42. Christian, J. T., Ladd, C. C., Baecher, G. B. (1994). "Reliability and probability in stability analysis". Journal of Geotechnical Engineering, ASCE, 120(12): 1071-1111.

43. Malkawi, A. I. H., Hassan, W. F., Abdulla, F. A. (2000). "Uncertainty and reliability analysis applied to slope stability". Journal of Structural Safety, 22(2): 161-187.

44. Low, B. K., Gilbert, R. B., Wright, S. G. (1998). "Slope reliability analysis using generalized method of slices". Journal of Geotechnical and Geoenvironmental Engineering, 124(4): 350-362.

45. John T. Christian (2004). "Geotechnical Engineering Reliability: How Well Do We Know What We Are Doing?" Journal of Geotechnical and Geo-environmental Engineering, 130(10), 985-1003.

46. Moore, R. E. (1996). "Interval analysis". Prentice-Hall, Englewood Cliffs, NJ.

47. Goodman, I. R., Nguyen, H. T. (1985). "Uncertainty models for Knowledge-based Systems; A Unified Approach to the Measurement of Uncertainty". New York, Elsevier Science Inc.

48. Foye, K. C., Salgado, R., and Scott, B. (2006). "Assessment of variable uncertainties for reliability-based design of foundations". Journal of Geotechnical and Geoenvironmental Engineering, 132(9).

49. Christian, J. T., and Baecher, G. B. (2001). Discussion on "Factors of safety and reliability in geotechnical engineering by J. M. Duncan," Journal of Geotechnical and Geoenvironmental Engineering, 127(8), 700–702.

50. Harr, M. E. (1987). "Reliability-Based Design in Civil Engineering". McGraw-Hill, New York.

51. Achintya Haldar and Sankaran Mahadevan, 2000. Probability, Reliability, and Statistical Methods in Engineering Design. John Wiley & Sons, Inc, pp.296.

52. Fishman, G. S. (1995). "Monte Carlo: Concepts, Algorithms, and Applications". Springer, New York.

53. Gordon A. Fenton and D.V. Griffiths (2008). "Risk assessment in Geotechnical Engineering". John Wiley & Sons Inc, pp. 435.

54. Rashad. Elrawy A. (2015). "Practical Application of Stochastic Methods in Geotechnical Engineering". Journal of Engineering Sciences, Assiut University Faculty of Engineering, Pp57-70.

55. Box, G.E.P. and Muller, M.E. (1958). A note on "the generation of random normal deviates". Annals of Mathematical Statistics, 29(2): 610-611.

56. Rocscience Inc. (2016). "Probabilistic analyses in Phase 2 8.0". Accessed on 09/15/2016, https://www.rocscience.com/help/phase2/webhelp/phase2.htm.

57. Gustavo A. Ordonez (2011). "SHAKE2000 a Computer Program for the 1D-Analysis of Geotechnical Earthquake Engineering Problems User's Manual". pp. 231.

58. L.H. Mejia and E.M. Dawson, 2006. Earthquake deconvolution for FLAC. 4th International FLAC Symposium on Numerical Modeling in Geomechanics, Paper: 04-10, pp. 9.

Eleyas Assefa, Dr. Li Jian Lin, Dr. Costas I. Sachpazis, Dr. Deng Hua Feng, Dr. Sun Xu Shu, and Xiaoliang Xu: "Slope Stability Evaluation for the New Railway Embankment using Stochastic Finite Element and Finite difference Methods" *Electronic Journal of Geotechnical Engineering*, 2017 (22.01), pp 51-79. Available at ejge.com

ΔΙΑΚΡΙΣΕΙΣ ΕΛΛΗΝΩΝ ΓΕΩΜΗΧΑΝΙΚΩΝ

The Electronic Journal of Geotechnical Engineering

EST. 1996

The Best of 2017: Top 10

Top 1 of 10

George Fernandes Azevedo, Hernán Eduardo Martínez Carvajal, Juan Felix Rodriguez Rebolledo, Newton Moreira de Souza, and André Pacheco de Assis: "Landslide Susceptibility Mapping Using GIS and Probabilistic Methods"

Top 2 of 10

Eleyas Assefa, Dr. Li Jian Lin, **Dr. Costas I. Sachpazis**, Dr. Deng Hua Feng, Dr. Sun Xu Shu, and Xiaoliang Xu: "Slope Stability Evaluation for the New Railway Embankment using Stochastic Finite Element and Finite Difference Methods"

Top 3 of 10

Liu Zhenping: "Application of Digital Image Deformation Measurement Technology into Face Rockfill Dam Shaking Table Model Test"

Top 4 of 10

Yulan Wang: "The application of anti-slide pile with anchor cable in the protection of a World Cultural Heritage Site of Ming-Jing Tai"

Top 5 of 10

Edy Purwanto: "Geotechnical Aspects of Bored Pile Construction on Clayshale"

Top 6 of 10

Carlos J. Sainea-Vargas: "Numerical and Probabilistic Analyses of Deep Excavations in Soft Soils" by Carlos J. Sainea-Vargas and Mario C. Torres-Suárez

Top 7 of 10

Desiani & Rahardjo: "Characterization of Bandung Soft Clay (by Characterization of Bandung Soft Clay)"

Top 8 of 10

Dr. Raju Sarkar: "Application of Soil Nailing for Landslide Mitigation in Bhutan: A Case Study at Sorchen Bypass"

Top 9 of 10

Søren Dam Nielsen: "Effect on the Grain Size Distribution when Preparing Sand Using Poker Vibrators"

Top 10 of 10

Aleksej Aniskin, Khrystyna Moskalova, and Željko Kos: "Wall Friction Angle of Grain Material With Respect to Dominant Particle Orientation"

ΠΡΟΣΕΧΕΙΣ ΓΕΩΤΕΧΝΙΚΕΣ ΕΚΔΗΛΩΣΕΙΣ

Για τις παλαιότερες καταχωρήσεις περισσότερες πληροφορίες μπορούν να αναζητηθούν στα προηγούμενα τεύχη του «περιοδικού» και στις παρατιθέμενες ιστοσελίδες.

5th International Course on Geotechnical and Structural Monitoring, 22 - 25 May 2018, in Rome www.geotechnicalmonitoring.com

EUROCK 2018 Geomechanics and Geodynamics of Rock Masses, 22-26 May 2018, Saint Petersburg, Russia, www.eurock2018.com/en

4th GeoShanghai International Conference, May 27-30, 2018, Shanghai, China, http://geo-shanghai.org

micro to MACRO - Mathematical Modelling in Soil Mechanics, May 29-June 1, 2018, Reggio Calabria, Italy, www.microtomacro2018.unirc.it

GeoReinforcement Workshop, 4 - 5 June 2018, Munich, Germany, https://igs.wufoo.com/forms/q10dk31u19dx00v/

International Conference on Deep Foundations and Ground Improvement - Urbanization and Infrastructure Development: Future Challenges, June 5-8, 2018, Rome, Italy, www.dfi.org/dfieventlp.asp?13310

GeoBarrier Workshop, 6 - 7 June 2018, Munich, Germany, https://igs.wufoo.com/forms/q10dk31u19dx00v/

XVI Danube-European Conference on Geotechnical Engineering: Geotechnical Hazards and Risks: Experiences and Practices, 7 - 9 June 2018, Skopje, Former Republic of Yugoslav www.decge2018.mk

16th European Conference on Earthquake Engineering (16thECEE), 18-21 June 2018, Thessaloniki, Greece, www.16ecee.org

CPT'18 4th International Symposium on Cone Penetration Testing, 21-22 June 2018, Delft, Netherlands, www.cpt18.org

PATA DAYS 2018 - 9th International INQUA Meeting on Paleoseismology, Active Tectonics and Archeoseismology, 24-29 June 2018, Chalkidiki, Greece, www.patadays2018.org

NUMGE 2018 9th European Conference on Numerical Methods in Geotechnical Engineering, 25-27 June 2018, Porto, Portugal, www.numge2018.pt

RockDyn-3 - 3rd International Conference on Rock Dynamics and Applications, 25-29 June 2018, Trondheim, Norway, www.rocdyn.org

ICOLD 2018 26th Congress – 86th Annual Meeting, 1 - 7 July 2018, Vienna, Austria, www.icoldaustria2018.com

9th International Conference on Physical Modelling in Geotechnics (ICPMG 2018), 17-20 July 2018, London, UK, www.icpmg2018.london

ICSSTT 2018 - 20th International Conference on Soil Stabilization Techniques and Technologies, July 19 - 20, 2018, Toronto, Canada, https://waset.org/conference/2018/07/toronto/ICSSTT

GeoChine 2018 - 5th GeoChina International Conference Civil Infrastructures Confronting Severe Weathers and Climate Changes: From Failure to Sustainability, July 23-25, , HangZhou, China, http://geochina2018.geoconf.org

UNSAT2018 The 7th International Conference on Unsaturated Soils, 3 - 5 August 2018, Hong Kong, China, www.unsat2018.org

China- Europe Conference on Geotechnical Engineering, 13-16 August 2018, Vienna, Austria, https://china-euro-geo.com

CRETE 2018 6th International Conference on Industrial & Hazardous Waste Management, 4-7 September 2018, Chania, Crete, Greece, www.hwm-conferences.tuc.gr

EUCEET 2018 - 4th International Conference on Civil Engineering Education: Challenges for the Third Millennium, 5-8 September 2018, Barcelona, Spain, http://congress.cimne.com/EUCEET2018/frontal/default.asp

SAHC 2018 11th International Conference on Structural Analysis of Historical Constructions "An interdisciplinary approach", 11-13 September 2018, Cusco, Perú http://sahc2018.com

26th European Young Geotechnical Engineers Conference, 11 - 14 September 2018, Reinischkogel, Austria, www.tugraz.at/en/institutes/ibg/events/eygec

11th International Conference on Geosynthetics (11ICG), 16 - 20 Sep 2018, Seoul, South Korea, www.11icg-seoul.org

CHALK 2018 Engineering in Chalk 2018, 17-18 September 2018, London, U.K., www.chalk2018.org

International Symposium on Energy Geotechnics SEG - 2018, 25-28 September 2018, Lausanne, Switzerland https://seg2018.epfl.ch

HYDRO 2018 - Progress through Partnerships, 15-17 October 2018, Gdansk, Poland, www.hydropower-dams.com/hydro-2018.php?c_id=88

GEC - Global Engineering Congress Turning Knowledge into Action, 22 - 26 October, London, United Kingdom, www.ice.org.uk/events/global-engineering-congress

ARMS10 - 10th Asian Rock Mechanics Symposium, ISRM Regional Symposium, 29 October - 3 November 2018, Singapore, www.arms10.org

ACUUS 2018 16th World Conference of Associated research Centers for the Urban Underground Space "Integrated Underground Solutions for Compact Metropolitan Cities", 5 – 7 November 2018, Hong Kong, China, www.acuus2018.hk

International Symposium Rock Slope Stability 2018, 13-15 November, 2018, Chambéty, France, www.c2rop.fr/symposium-rss-2018

GeoMEast 2018 International Congress and Exhibition: Sustainable Civil Infrastructures, 24 - 28 November 2018, Cairo, Egypt, www.geomeast.org

WTC2019 Tunnels and Underground Cities: Engineering and Innovation meet Archaeology, Architecture and Art and ITA - AITES General Assembly and World Tunnel Congress, 3-9 May 2019, Naples, Italy, www.wtc2019.com

14th international Conference "Underground Construction", 3 to 5 June 2019, Prague, Czech Republic, www.ucprague.com

2019 Rock Dynamics Summit in Okinawa, 7-11 May 2019, Okinawa, Japan, www.2019rds.org

VII ICEGE ROMA 2019 - International Conference on Earthquake Geotechnical Engineering, 17 - 20 June 2019, Rome, Italy, www.7icege.com

ICONHIC2019 - 2nd International Conference on Natural Hazards and Infrastructure, 23-26 June 2019, Chania, Crete Island, Greece, https://iconhic.com/2019/conference

IS-GLASGOW 2019 - 7th International Symposium on Deformation Characteristics of Geomaterials, 26 - 28 June 2019, Glasgow, Scotland, UK, https://is-glasgow2019.org.uk

cmn 2019 -Congress on Numerical Methods in Engineering, July 1 - 3, 2019, Guimarães, Portugal, www.cmn2019.pt

For additional information, please contact the secretariat of the congress, Ms. Lara Leite

CMN2019, Universidade do Minho, Departamento de Engenharia Civil, 4800-058 Guimarães - Portugal
Email: cmn2019@civil.uminho.pt
Telephone: +351 253 510 748
Fax: +351 253 510 217

The 17th European Conference on Soil Mechanics and Geotechnical Engineering, 1st - 6th September 2019, Reykjavik Iceland, www.ecsmge-2019.com

14th ISRM International Congress, 13-18 September 2019, Iguassu Falls, Brazil, www.isrm2019.com

☙ ❧

XVII African Regional Conference on Soil Mechanics and Geotechnical Engineering
07-10 October 2019, Cape Town, South Africa

The South African Institution of Civil Engineering cordially invites all our colleagues from Africa and beyond to attend the 17th African Regional Conference on Soil Mechanics and Geotechnical Engineering.

Hosted in one of the continent's most iconic cities, this conference will serve practitioners, academics and students of all geotechnical backgrounds. The conference will take place at the Cape Town International Convention Centre (CTICC) offering world class conferencing facilities in the heart of South Africa's mother city and will offer extensive opportunities for Technical Committee Meetings, Workshops, Seminars, Exhibitions and Sponsorships. Exciting Technical Visits, including tours to the famous Robben Island, await.

The 7th African Young Geotechnical Engineers' Conference (8 – 10 October 2019) will commence on 8 October 2019, the day following the African Regional Conference (ARC) opening. The conference venue will be shared with the ARC delegates to initiate dialogue between junior and senior engineers while young geotechnical engineers acquaint themselves with the industry standards, new geotechnical developments and resources available to further their careers. The YGE conference provides an approachable audience within a vibrant environment where young presenters under the age of 35 are encouraged to exercise their presentation and technical writing skills on a continental platform.

Organiser: SAICE
Contact person: Dr Denis Kalumba
Email: denis.kalumba@uct.ac.za

☙ ❧

XVI Asian Regional Conference on Soil Mechanics and Geotechnical Engineering, 21 - 25 October 2019, Taipei, China www.16arc.org

XVI Panamerican Conference on Soil Mechanics and Geotechnical Engineering, 18-22 November 2019, Cancun, Quintana Roo, Mexico, http://panamerican2019mexico.com/panamerican

☙ ❧

YSRM2019 - the 5th ISRM Young Scholars' Symposium on Rock Mechanics
and
REIF2019 - International Symposium on Rock Engineering for Innovative Future
1-4 December 2019, Okinawa, Japan

Contact Person: Prof. Norikazu Shimizu, jsrm-office@rocknet-japan.org

☙ ❧

Nordic Geotechnical Meeting
27-29 May 2020, Helsinki, Finland

Contact person: Prof. Leena Korkiala-Tanttu
Address: SGY-Finnish Geotechnical Society,
Phone: +358-(0)50 312 4775
Email: leena.korkiala-tanttu@aalto.fi

☙ ❧

EUROCK 2020
Hard Rock Excavation and Support
June 2020, Trondheim, Norway

Contact Person: Henki Ødegaard, henki.oedegaard@multiconsult.no

☙ ❧

EURO GEO WARSAW 2020 7 6-9 SEPTEMBER

www.eurogeo7.org

We are pleased to invite you to the 7th EuroGeo conference, to be held in Warsaw, Poland in 2020. Poland is a country with more than a thousand years of recorded history and has a strong European identity. The country was first to free itself from communist domination in 1989 and is now fully democratic and a member of the European Union. Poland is a leader in infrastructure development in the region, which has resulted in many extraordinary projects. Warsaw, with its central location, is an ideal base for exploring the country. Today, the city is a dynamic cultural and business centre, with strong links not only to Western Europe but also to the East. PSG-IGS, a Polish Chapter of IGS is young but thriving organization successfully cooperating with several chapters within Central Europe. It is an honour to host such a prestigious conference in Warsaw and We sincerely believe that the sessions will prove to be a success. Come to Warsaw, bring your family and enjoy your stay in our capital and help us to make this Conference not only scientifically profitable but also an unforgettable event.

Contact: eurogeo7inpoland@gmail.com

6th International Conference on Geotechnical and Geophysical Site Characterization
07-09-2020 ÷ 11-09-2020, Budapest, Hungary
www.isc6-budapest.com

Organizer: Hungarian Geotechnical Society
Contact person: Tamas Huszak
Address: Muegyetem rkp. 3.
Phone: 0036303239406
Email: huszak@mail.bme.hu
Website: http://www.isc6-budapest.com
Email: info@isc6-budapest.com

ΕΝΔΙΑΦΕΡΟΝΤΑ ΓΕΩΤΕΧΝΙΚΑ ΝΕΑ

68 Dams Collapse in China Every Year

A picture of the Three Gorges dam discharging floodwaters. The safety of reservoirs located across China remain a challenge.

As the debate about the Three Gorges dam rages on, on June 1, E. Jingping, Secretary General of the State Flood Control and Drought Relief Headquarters and Vice Minister of Water Resources, said that the safety of reservoirs continues to remain a challenge and is a weak link in this year's flood prevention efforts. As of last year, an average of 68 reservoir dams collapse every year in China.

He said, "The extent of casualties and economic cost from a dam collapsing possibly surpasses that of a natural disaster like a tsunami or a strong earthquake, and is no less damaging than a local war."

At present, China has 85,160 reservoirs. From 1954 to 2005, a total of 3,486 reservoir dams collapsed. Each year, many reservoirs experience flood damage. In 2004 alone, 7,286 reservoirs experienced flood damage and are in need of repair.

According to China Newsweek reports, among the 85,000 plus reservoirs in China, over 30,000 (35 percent) have problems but continue to be operational, constituting a major hidden danger in water resource facilities.

Now, in China, not one province, city, or district is free of dangerous reservoirs. In the provinces of Hunan, Guangdong, Sichuan, Shandong, Yunnan, Hubei, and Jiangxi, each province has more than 1,600 dangerous reservoirs. In Guangdong Province, there are 3,685 dangerous reservoirs—a total of 55 percent of all reservoirs in the province.

Dangerous reservoirs are usually located upstream from cities at the county level and above in China's administrative system. For nearby areas that have a large difference in elevation, the safety, resources, cities, industries, and public facilities of the people downstream will be directly affected.

Those currently under threat include 25.4 percent of China's cites with 179 dangerous reservoirs, and 16.7 percent of county towns with 285 such reservoirs. The urban and rural populations living in the above-mentioned areas account for 146 million people. In total, 8.8 million hectares of cultivated land is under threat.

In the world's record of disasters due to human technical failures, the 1975 collapse of China's Banqiao reservoir dam in Henan province ranked first, which is higher than the Chernobyl disaster in the former Soviet Union. In a matter of days, 26 dams collapsed one after another, which resulted in massive flooding in nine counties and one town. More than 100,000 corpses were retrieved when the flooding receded. Deaths due to the repercussions of grain shortages and infectious diseases amounted to 140,000; while the total number of deaths recorded was 240,000. This death toll was comparable to the China's Tangshan earthquake in the following year, and the damage dealt was worse than the collapse of Egypt's Aswan reservoir dam.

(Epoch Time Staff, June 11, 2006, https://www.theepochtimes.com/68-dams-collapse-in-china-every-year_1731001.html)

cs ω

Geosynthetica's 2017 Top 10 Stories

Each year we look back at the most-popular reads on Geosynthetica to gauge trends in the field and international reader interests. It also provides us another piece to add to the geosynthetics industry's historical record. While we find a diverse range of topics in our 2017 Top 10 (most-read) stories, we also find key connections between them.

Notably, articles on MSE reinforcement design and industry consolidation were prominent.

Paul C. Frankenberger, P.E.; Matthew M. Merritt, P.E.; and Mark Myers, P.E.'s article on "Secondary Geogrid Reinforcement in MSE Walls" was one of the most-read stories on Geosynthetica in 2017.

MSE design and performance occupied, in fact, the top three spots in the 2017 Top 10 List. On the topic of industry consolidation, three more of the ten most-read stories were about company or asset acquisitions.

NOTE: The list below is limited to articles originally published in 2017. If we open the list to articles that were first published in other years, we actually would find a fewer older stories in the 2017 Top 10 List. These stories pertain to geotechnical software, industry events (2016 – 2018), and stress cracking in geomembranes. That last article was in fact first published in 2002 and continues to be a top 10 story each year. (The article is currently being updated for a

2018 publication.)

GEOSYNTHETICA'S 2017 TOP 10 STORIES

The titles below are listed in order of rank, beginning with the most-viewed:

FHWA Limit Equilibrium Design Framework for MSE Structures
(February 28)

MSE Wall Failures vis-à-vis the Lack of Geotechnical Filters
(July 3)

Secondary Geogrid Reinforcement in MSE Walls
(April 10)

EXCLUSIVE: Video Interview with Solmax on Acquiring GSE Environmental
(December 20)

Reinforcing India's First Vertical Expansion of a Landfill
(June 1)

Solmax Establishes Solmax USA in Houston
(February 22)

Best Practices for Minimizing Geomembrane Wrinkling
(June 6)

Geosynthetics Apps for iPhone and Android Smartphones
(March 20)

Hanes Geo Acquires Terrafix in Geosynthetics Growth Move
(January 9)

270m-Long Reinforced Soil Structure for a South African Highway
(July 27)

Catrin Tarnowski's article on "Best Practices for Minimizing Geomembrane Wrinkles" was the 7th most-read story in 2017.

JUST MISSING OUT ON THE 2017 TOP 10 LIST

Narrowly edged out for a Top 10 spot was "Lime-Stabilized Backfill in MSE Retaining Structures", which was published on February 9. We mention it along with the 2017 Top 10 because it underscores just how important MSE design and performance was to Geosynthetica's international readers during the year.

(Chris Kelsey / Geosynthetica, January 4, 2018, https://www.geosynthetica.net/geosynthetica-2017-top-10-stories)

Final report details reasons behind Oroville Dam spillway incident

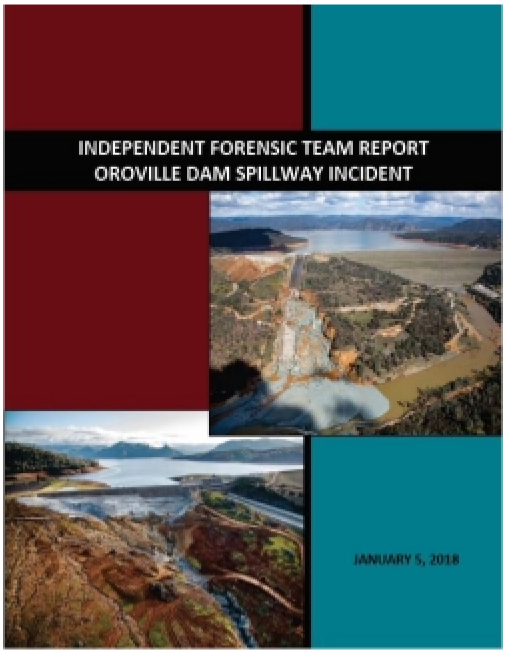

http://npdp.stanford.edu/sites/default/files/other_materials/independent_forensic_team_report_final_01-05-18_-_copy.pdf

Below are some telling statements surrounding the spillway incidents at Oroville Dam in California, U.S., that occurred in February 2017:

"The Oroville Dam spillway incident was caused by a long-term systemic failure of the California Department of Water Resources (DWR), regulatory, and general industry practices to recognize and address inherent spillway design and construction weaknesses, poor bedrock quality and deteriorated service spillway chute conditions."

"The incident cannot reasonably be 'blamed' mainly on any one individual, group, or organization."

Nonetheless, "Challenging current assumptions on what constitutes 'best practice' in our industry is overdue."

Final report released

In its final report, officially released today (from which the quotes above were taken), the Oroville Dam Spillway Incident Independent Forensic Team said there was no single root cause of the incident, nor was there a simple chain of events leading ultimately to the necessity of the evacuation order. "Rather, the incident was caused by a complex interaction of relatively common physical, human, organizational, and industry factors, starting with the design of the project and continuing until the incident."

Physical factors were placed in two general categories:

- Inherent vulnerabilities in the spillway design and as-constructed conditions, and subsequent chute slab deterioration
- Poor spillway foundation conditions in some locations

Human, organizational and industry factors were cited as:

- "Normalization" of drain flows and cracking in repeated inspections (starting in the early 1970s after initial slab cracking and high drain flows in the late 1960s)

- Decision (in February 2017) to accept use of emergency spillway against civil/geological advice

In the end, the team determined "There were many opportunities to intervene and prevent the incident, but the overall system of interconnected factors operated in a way that these opportunities were missed."

Specific to DWR, the report says:

"The dam safety culture and program within DWR … was still relatively immature at the time of the incident and has been too reliant on regulators and the regulatory process."

"… DWR has been somewhat overconfident and complacent regarding the integrity of its civil infrastructure and has tended to emphasize shorter-term operational considerations … [resulting] in strained internal relationships and inadequate priority for dam safety."

Lessons learned

In the end, the lessons learned are probably the most important take-away from the incident and provide a way forward for dam safety worldwide. They are:

- Dam owners must develop and maintain mature dam safety management programs which are based on a strong "top-down" dam safety culture. There should be one executive specifically charged with overall responsibility for dam safety, and this executive should be fully aware of dam safety concerns and prioritizations through direct and regular reporting from a designated dam safety professional, to ensure that "the balance is right" in terms of the organization's priorities.
- More frequent physical inspections are not always sufficient to identify risks and manage safety.
- Periodic comprehensive reviews of original design and construction and subsequent performance are imperative. These reviews should be based on complete records and need to be more in-depth than periodic general reviews, such as the current FERC-mandated five-year reviews.
- Appurtenant structures associated with dams, such as spillways, outlet works, power plants, etc., must be given attention by qualified individuals. This attention should be commensurate with the risks that the facilities pose to the public, the environment, and dam owners, including risks associated with events which may not result in uncontrolled release of reservoirs, but are still highly consequential.
- Shortcomings of the current Potential Failure Mode Analysis (PFMA) processes in dealing with complex systems must be recognized and addressed. A critical review of these processes in dam safety practice is warranted, comparing their strengths and weaknesses with risk assessment processes used in other industries worldwide and by other federal agencies. Evolution of "best practice" must continue by supplementing current practice with new approaches, as appropriate.
- Compliance with regulatory requirements is not sufficient to manage risk and meet dam owners' legal and ethical responsibilities.

Bottom line

As the report succinctly states:

"The fact that this incident happened to the owner of the

tallest dam in the United States, under regulation of a federal agency, with repeated evaluation by reputable outside consultants, in a state with a leading dam safety regulatory program, is a wake-up call for everyone involved in dam safety."

(Elizabeth Ingram, Managing Editor / HYDROWORLD.com, 01/05/2018, https://www.hydroworld.com/articles/2018/01/breaking-news-final-report-details-reasons-behind-oroville-dam-spillway-incident.html?cmpid=enl_hydroworld_hydro_updates_2018-01-09&pwhid=a772c9b9feb108b3ca3aff76e7a549b589909d83db1c9019a5d2be06d2fcab93d6b56e362a9d02a8d3c052ad9d8f5d721ca4ad850446c554937a76cc88c7d911&eid=294526711&bid=1967388)

Deadly California mudslides show the need for maps and zoning that better reflect landslide risk

Scenic hill slopes can be inspiring – or deadly, as we are seeing after the disastrous debris flows that have ravaged the community of Montecito, California in the wake of heavy rains on Tuesday, Jan. 9, 2018. At least 20 people are dead, and four remain missing. More than a hundred buildings have been destroyed or damaged by moving walls of mud and boulders that rumbled down creeks and canyons into houses and roads.

As mountains rise, erosion tears them down. And Southern California's mountains are rising fast, squeezed up by the action of the region's active faults. This produces steep slopes that erode quickly, though much of that erosion happens in infrequent events, such as big rainstorms right after big wildfires.

We know that risks vary across the terrain and that some places in landslide-prone zones are more dangerous than others. In some regions the riskiest areas are well downslope or downstream of slide-prone slopes, in the places where debris runs out and comes to rest. Unfortunately, few people are aware of these risks when developers build in and around landslide-prone mountains.

A predictable disaster

The U.S. Geological Survey estimates that landslides kill 25 to 50 people a year in the United States – more than earthquakes or volcanoes. Yet landslides receive far less attention and research funding than other natural hazards.

Part of the problem is that when a large earthquake strikes, the whole region feels it. But landslides tend to impact localized areas, so they rarely attract widespread attention, except in devastating cases like Montecito. Furthermore, different kinds of landslides present very different hazards. Assessing landslide risks requires an understanding of how erosional processes shape Earth's surface in different regions.

In a general sense, the threat to Montecito was clear. Scientists and planners have known for decades that the mountains of Southern California are shaped by a cycle of fire, rain and debris flows. Back in 1989, when I was a graduate student studying landslides, journalist John McPhee published his acclaimed book "The Control of Nature." In it, McPhee described scenes of devastation resulting from intense rainfall running off of wildfire-charred slopes to roar down canyons around Los Angeles.

Landslides | National Geographic,
https://www.youtube.com/watch?time_continue=158&v=mknStAMia0Q

The Montecito disaster did not come as a complete surprise. Indeed, the U.S. Geological Survey warned of high potential for disastrous landslides if intense rain fell on mountainsides around Santa Barbara that had been scorched by the Thomas wildfire in December. When that perfect storm landed, it hit bare, baked soil that could not readily absorb water. So the rain ran off, picking up soil, boulders and debris as it surged down canyons and streams. These debris-charged torrents slowed only where steep channels gave way to gentler slopes.

Most of the damage occurred along the run-out pathways of the debris flows – areas where material can flow after it starts sliding downhill. Yet landslide hazard maps generally don't show predicted run-out zones. Instead, they typically show only the locations of the source areas where landslides are likely to start.

Better information for residents

There are reasons why people keep building homes in landslide-prone areas. Some decide it's worth the risk. In Seattle, where I live, steep slide-prone slopes tend to offer the best, and most expensive, views. Conversely, in low-income regions such as Appalachia and many developing countries, the poor often are pushed up onto potentially unstable hillsides. Generally, however, I suspect that many Americans living in landslide country are simply unaware of potential hazards that the lay of the land presents to their homes, neighborhoods and businesses.

Sometimes politics or greed plays a role. After Hurricane Frances hammered North Carolina in 2004, the state legislature approved a program to map landslide hazards. But once the first maps were produced, the program was canceled over concerns that the maps would affect land values and be used to regulate development.

Without this kind of information, residents are physically and financially exposed. "Earth movement," such as landslides, generally is not covered by homeowner's insurance policies. And by the time a landslide comes, developers are long gone, leaving homeowners holding the bag.

Upper part of the Oso, Washington landslide site, photographed April 8, 2014 (see small house just inside treeline at lower left for scale).

And, of course, different types of landslides pose different risks. In the slow-moving Rattlesnake Ridge landslide in central Washington state, a 20-acre parcel of land is sliding downhill about a foot and half per week. Residents have been moved out of the at-risk zone, and engineers and geologists are monitoring the site in real time to evaluate and update hazard assessments.

In contrast, the Oso landslide north of Seattle on March 22, 2014 was so large and fast-moving that even a real-time warning would not have prevented tragedy. This disaster killed 43 people in a couple of minutes when an entire hillside collapsed. In response, Washington state has started posting detailed topographical maps online for use in identifying areas at risk for generating landslides. But hazard maps still don't identify potential downhill run-out zones.

It's time to get serious about landslide zoning, in the way that the federal government maps areas at serious risk of flooding. Landslide hazard maps delineating potential run-out zones should be part of local land use planning. These maps could help guide zoning decisions and better inform homeowners, banks and insurance companies of potential risks. Ultimately, the best way to reduce landslide risk is to avoid building things we value in places where run-out is likely. For when there's no controlling nature, there's only living with her.

(David R. Montgomery, Professor of Earth and Space Sciences, University of Washington / THE CONVERSATION, January 16, 2018, https://theconversation.com/deadly-california-mudslides-show-the-need-for-maps-and-zoning-that-better-reflect-landslide-risk-90087)

ΕΝΔΙΑΦΕΡΟΝΤΑ - ΣΕΙΣΜΟΙ

Rates of great earthquakes not affected by moon phases, day of year

There is an enduring myth that large earthquakes tend to happen during certain phases of the Moon or at certain times during the year. But a new analysis published in *Seismological Research Letters* confirms that this bit of earthquake lore is incorrect.

After matching dates and lunar phases to 204 earthquakes of magnitude 8 or larger, Susan Hough of the U.S. Geological Survey concluded that there is no evidence that the rates of these great earthquakes are affected by the position of the Earth relative to either the Moon or the Sun.

In fact, the patterns that some observers see as linking large earthquakes with specific parts of the lunar cycle "are no different from the kinds of patterns you would get if the data are completely random," Hough noted.

To determine this, Hough looked at both the day of the year and the lunar phase for 204 large earthquakes from the global earthquake catalog, dating back to the 1600s. To avoid detecting clusters of earthquakes within the data that are related to other factors, she chose to look at larger earthquakes because they are less likely to be an aftershock of a bigger earthquake.

Looking at only large earthquakes also allowed Hough to pare down the list to a manageable number that could be matched to lunar phase information found in online databases.

Her analysis did turn up some clusters of earthquakes on certain days, but to test for any significance in the patterns she was observing, she randomized the dates of the earthquakes to find out what kind of patterns would appear in these random data. The patterns in the random data were no different from the kinds of patterns showing up in the original data set, she found.

This isn't an unusual finding, Hough noted. "When you have random data, you can get all sorts of apparent signals, just like when you flip a coin, you sometimes end up with five heads in a row."

Hough did see some unusual "signals" in the original data; for instance, the highest number of earthquakes (16) occurring on a single day came seven days after the new moon. But this signal was not statistically significant, "and the lunar tides would be at a minimum at this point, so it doesn't make any physical sense," she noted.

Hough said that the Moon and Sun do cause solid Earth tidal stresses— ripples through the Earth itself, and not the waters hitting the coastline—and could be one of the stresses that contribute in a small way to earthquake nucleation."

Some researchers have shown that "there is in some cases a weak effect, where there are more earthquakes when tidal stresses are high," she said, "But if you read those papers, you'll see that the authors are very careful. They never claim that the data can be used for prediction, because the modulation is always very small."

The idea that the Sun and Moon's positions in the sky can modulate earthquake rates has a long history, she said. "I've read Charles Richter's files, the amateur predictors who wrote to him in droves, because he was the one person that people knew to write to ... and if you read the letters, they're similar to what people are saying now, it's all the same ideas."

"Sooner or later there is going to be another big earthquake on a full moon, and the lore will pop back up," said Hough. "The hope is that this will give people a solid study to point to, to show that over time, there isn't a track record of big earthquakes happening on a full moon."

More information: "Do Large (Magnitude ? 8) Global Earthquakes Occur on Preferred Days of the Calendar Year or Lunar Cycle?" *Seismological Research Letters* (2018). DOI: 10.1785/0220170154

(January 16, 2018, https://phys.org/news/2018-01-great-earthquakes-affected-moon-phases.html)

ΕΝΔΙΑΦΕΡΟΝΤΑ - ΓΕΩΛΟΓΙΑ

Photo Timeline: How the Earth Formed
The evolution of the Earth

Take a tour through the fascinating geologic record left behind by the major milestones in Earth's 4.5 billion years. Here, we focus on the events that shaped the planet's surface, such as giant impacts and its oxygen-rich atmosphere.

Earth forms

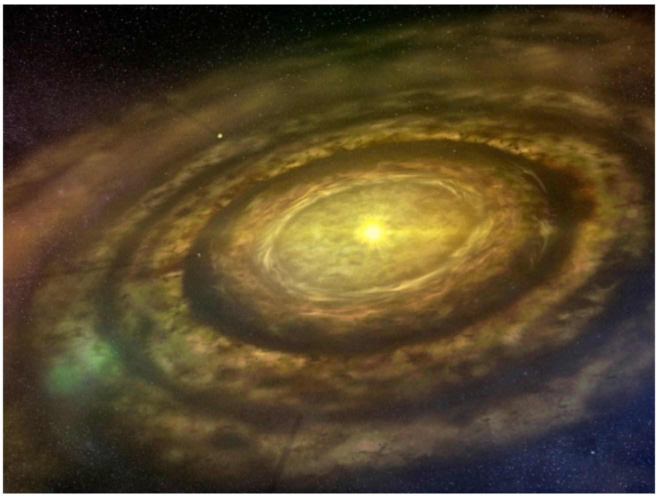

It's hard to know when the Earth first formed, because no rocks have survived from the planet's earliest days. While scientists disagree on the details, most researchers think Earth formed by a series of collisions that took place less than 100 million years after the solar system coalesced. More than 10 impacts with other bodies added bulk to our growing planet, according to most models of Earth's formation. By measuring the age of rocks on the moon, and meteorites found on Earth, scientists estimate the Earth consolidated by 4.54 billion years ago. The young planet had established an atmosphere and iron core, when …

Boom! Earth-Moon collision

The final collision in Earth's timeline was with Theia, a rocky planetoid perhaps the size of Mars. This protoplanet sideswiped Earth, leaving our planet mostly intact but destroying itself and blowing away Earth's atmosphere. Theia's vaporized debris condensed into Earth's moon. Some researchers think remnants of the pre-collision Earth still exist deep in Earth's mantle and outer core today. The mantle is the layer between the surface crust and the core.

Magma ocean

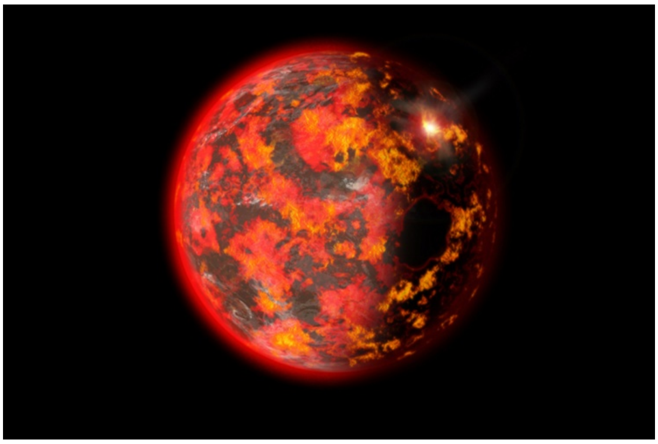

The force of the moon-forming impact left Earth a churning hot magma blob. The hellish conditions meant Earth resembled Venus for a time, with a hazy, steamy atmosphere. But as the planet cooled, lava became rock and liquid water started to condense, forming Earth's first ocean. The oldest minerals found on Earth, called zircons, date back to this time and are 4.4 billion years old.

First continents

Today, Earth is completely covered by giant tectonic plates of continental and oceanic crust. But the young Earth's first tectonic plates were much smaller. These protocontinents were recycled volcanic rock that had been remelted, or also buried and converted to metamorphic rock. These metamorphic belts often contain rich deposits of gold, silver, copper and other precious metals. The Earth's new crust grew rapidly, with about 70 percent of the crust formed by 3 billion years ago, researchers think. The earliest chemical markers of life also appeared with the first continents, about 3.8 billion years ago.

Breath of life

The first whiffs of oxygen — from the evolution of photosynthesis — emerged in rocks about 3.5 billion years ago. Photosynthesis was one of

Boring billion

After atmospheric oxygen levels spiked 2.4 billion years ago, not much happened on Earth for another billion years. Earth was so staid that scientists call this stretch of time the "boring billion." Things were pretty quiet tectonically, too: The continents were stuck in a supercontinental traffic jam for most of the boring billion. Many researchers think there's a link between the lack of tectonic activity and the boring billion — perhaps life needed a kick from drifting continents to drive evolution past photosynthesis, toward complex bodies.

(Becky Oskin, Senior Writer / LIVESCIENCE,| June 30, 2014, https://www.livescience.com/46593-how-earth-formed-photo-timeline.html)

ᴓᴓ

1.7-Billion-Year-Old Chunk of North America Found Sticking to Australia

Geologists matching rocks from opposite sides of the globe have found that part of Australia was once attached to North America 1.7 billion years ago.

Researchers from Curtin University in Australia examined rocks from the Georgetown region of northern Queensland. The rocks — sandstone sedimentary rocks that formed in a shallow sea — had signatures that were unknownin Australia but strongly resembled rocks that can be seen in present-day Canada.

The researchers, who described their findings online Jan. 17 in the journal Geology, concluded that the Georgetown area broke away from North America 1.7 billion years ago. Then, 100 million years later, this landmass collided with what is now northern Australia, at the Mount Isa region.

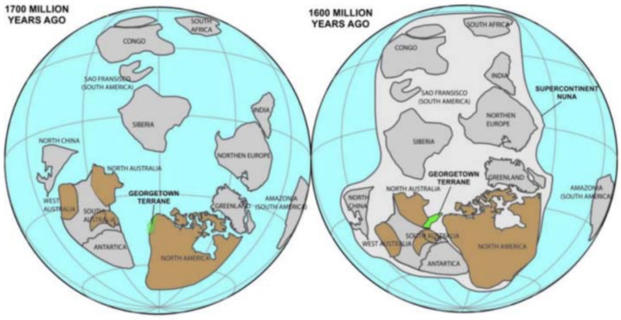

This diagram shows the Georgetown terrane, in green, joining Australia around 1.6 billion years ago during the formation of the supercontinent Nuna.

"This was a critical part of global continental reorganization when almost all continents on Earth assembled to form the supercontinent called Nuna," Adam Nordsvan, Curtin University doctoral student and lead author of the study, said in a statement.

Nordsvan added that Nuna then broke apart some 300 million years later, with the Georgetown area stuck to Australia as the North American landmass drifted away.

The continents as we know them today have shifted places throughout Earth's 4-billion-year history. Most recently, these landmasses came together to form the supercontinent known as Pangaea about 300 million years ago. Geologists are still trying to reconstruct how even earlier supercontinents assembled and broke apart before Pangaea. Scientists first proposed the existence of Nuna, Earth's first supercontinent, in 2002. Nuna is sometimes called Columbia.

Previous research suggested that northeast Australia was near North America, Siberia or North China when the continents came together to form Nuna, Nordsvan and colleagues noted, but scientists had yet to find solid evidence of this relationship.

These rocks found around Georgetown, Australia, are made from sediments originally deposited off the coast of present-day Canada.

Colliding landmasses can form mountain ranges. For example, the clash of the continental plates of India and Asia about 55 million years ago created the Himalayas. The researchers of the new study say they found evidence of mountains forming when Georgetown rammed into the rest of Australia.

"Ongoing research by our team shows that this mountain belt, in contrast to the Himalayas, would not have been very high, suggesting the final continental assembling process that led to the formation of the supercontinent Nuna was not a hard collision like India's recent collision with Asia,"Zheng-Xiang Li, a co-author of the study and a professor of Earth science at Curtin University, said in the statement.

Original article on Live Science*.*

(Megan Gannon / Live Science, January 22, 2018, https://www.livescience.com/61490-chunk-of-north-america-in-australia.html)

Laurentian crust in northeast Australia: Implications for the assembly of the supercontinent Nuna

Adam R. Nordsvan, William C. Collins, Zheng-Xiang Li, Christopher J. Spencer, Amaury Pourteau, Ian W. Withnall, Peter G. Betts, Silvia Volante

Geology (2018) DOI: https://doi.org/10.1130/G39980.1, Published: January 17, 2018

The Georgetown Inlier of northeast Australia provides evidence of critical links between Australia and Laurentia during the late Paleoproterozoic and the early Mesoproterozoic. Detrital zircon age spectra from sedimentary strata within the inlier show two distinct changes in sedimentary provenance: (1) the lowermost units (depositional age ca. 1700–1650 Ma) have detrital zircon age spectra that strongly resemble Laurentian magmatic ages and detrital zircon age spectra of the similar-aged Wernecke Supergroup of northwest Laurentia; (2) sediments deposited from ca. 1650 to 1610 Ma show a unimodal proximal signature; and (3) postorogenic sediments deposited after 1550 Ma have detrital zircon age spectra like the Mount Isa Inlier of the North Australia craton. Along with new paleocurrent measurements, the detrital age data challenge current models that suggest that the Georgetown Inlier was part of Australia before ca. 1700 Ma. Rather, we argue it was a continental ribbon rifted from west Laurentia during slab rollback ca. 1680 Ma; by 1650 Ma, the Georgetown Inlier had completely separated from Laurentia, and ca. 1600 Ma collided with Australia during supercontinent Nuna amalgamation.

https://pubs.geoscienceworld.org/gsa/geology/article-abstract/526080/laurentian-crust-in-northeast-australia?redirectedFrom=fulltext

Curtin researchers discover a piece of America in northern Australia

Curtin University researchers have discovered rocks in northern Queensland that bear striking similarities to those found in North America, suggesting that part of northern Australia was actually part of North America 1.7 billion years ago.

The research paper in *GEOLOGY* published by the Geological Society of America, concluded that the rocks found in Georgetown, 412 kilometres west of Cairns, have signatures that are unknown in Australia and instead have a surprising resemblance to rocks found in Canada today.

Curtin University PhD student Adam Nordsvan from the School of Earth and Planetary Sciences said the findings were significant as they unlock important information about the 1.6 billion year old supercontinent Nuna.

"Our research shows that about 1.7 billion years ago, Georgetown rocks were deposited into a shallow sea when the region was part of North America. Georgetown then broke away from North America and collided with the Mount Isa region of northern Australia around 100 million years later," Mr Nordsvan said.

"This was a critical part of global continental reorganisation when almost all continents on Earth assembled to form the supercontinent called Nuna.

"The team was able to determine this by using both new sedimentological field data and new and existing geochronological data from both Georgetown and Mount Isa to reveal this unexpected information on the Australia continent."

Researchers then determined that when the supercontinent Nuna broke apart an estimated 300 million years later, the Georgetown area did not drift away and instead became a new piece of real estate permanently stuck to Australia.

Co-author John Curtin Distinguished Professor Zheng-Xiang Li, also from Curtin's School of Earth and Planetary Sciences, said the research also revealed new evidence of mountains being built in both the Georgetown region and Mt Isa when Georgetown collided with the rest of Australia.

"Ongoing research by our team shows that this mountain belt, in contrast to the Himalayas, would not have been very high, suggesting the final continental assembling process that led to the formation of the supercontinent Nuna was not a hard collision like India's recent collision with Asia," Professor Li said.

"This new finding is a key step in understanding how Earth's first supercontinent Nuna may have formed, a subject still being pursued by our multidisciplinary team here at Curtin University."

The research was co-authored by researchers from Curtin University, Monash University, and the Geological Survey of Queensland.

MEDIA RELEASE, Friday 19 January 2018

http://news.curtin.edu.au/media-releases/curtin-researchers-discover-piece-america-northern-australia/

ΕΝΔΙΑΦΕΡΟΝΤΑ - ΠΕΡΙΒΑΛΛΟΝ

Απίστευτη εικόνα στον ουρανό της Κρήτης

Μία απίστευτη εικόνα κατέγραψε ο φωτογραφικός φακός του Γιάννη Γκίκα από τον ουρανό της Κρήτης.

Πρόκειται για ένα φακοειδές νέφος που σχηματίστηκε στο Ρέθυμνο και δημοσιεύθηκε από την Ειρήνη Καλαϊτζάκη στους «Μετεωκρήτες».

Το φακοειδές νέφος σχηματίζεται σε μεγάλο υψόμετρο και κάθετα προς την κατεύθυνση του ανέμου ενώ όπως ενημερώνει η κ. Καλαϊτζάκη σε σχετική ανάρτησή της η συγκεκριμένη περιοχή του Ρεθύμνου έχει δώσει και στο παρελθόν τέτοια νέφη εξαιτίας των νοτίων ανέμων.

(12 Ιανουαριου 2018, https://www.cretapost.gr/382255/apistefti-ikona-ston-ourano-tis-kritis-dite-ti-schimatistike)

Magnetic liquid window helps buildings keep their cool

Researchers at Germany's University of Jena have developed a new type of window that uses switchable magnetic particles suspended in liquid to create shade and capture heat energy.

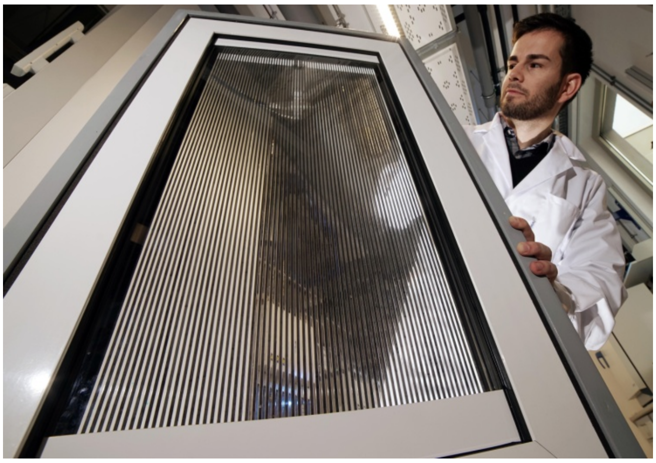

The prototype window is a suspended particle device (SPD) where iron nanoparticles are circulated in a liquid between a laminate of structured, rolled glass and a thin cover with high surface strength. Each laminate contains multiple channels a few millimetres wide through which the liquid flows. The capture and release of particles happens in a separate tank, so an electrical connection at the window isn't required. According to the researchers, the low thickness of the SPD of typically 4–6mm allows for integration with standard double or triple glazing.

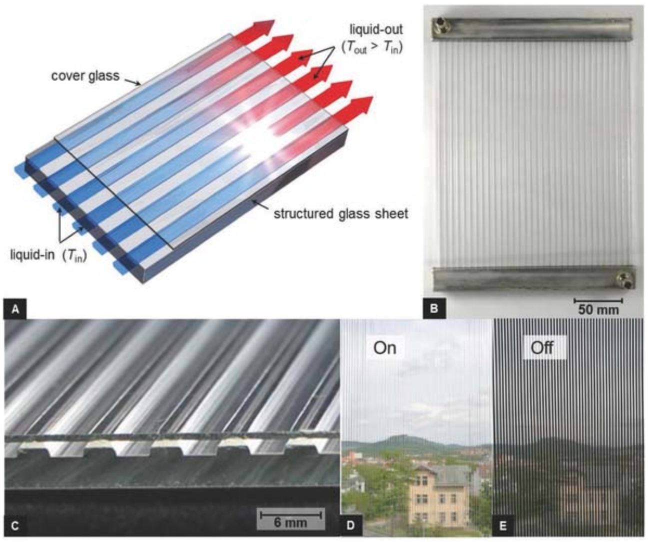

Light permeability can be altered at the touch of a button, and when fully shaded the device has a claimed solar thermal harvesting efficiency in the region of 45 per cent. Published in the journal *Advanced Sustainable Sys-*

tems (https://onlinelibrary.wiley.com/doi/full/10.1002/adsu.201700140), the research holds promise for significantly improving the efficiency of buildings by both reducing cooling loads and generating heat for use elsewhere.

"Depending on the number of the iron particles in the liquid, the liquid itself takes on different shades of grey, or it will even turn completely black," said Lothar Wondraczek, chair of glass chemistry at the University of Jena and the project's coordinator.

"Then, it becomes possible to automatically adjust the incidence of light, or to harvest solar heat which can then be put to further use within the building."

The research is part of the EU's Horizon 2020 programme and has received almost €6m in EU funding over the past two years, as well as an additional €2.2m from industrial partners. Current prototypes were manufactured on a scale of around 200 square meters, and the first commercial applications of the technology are planned for later this year.

(the engineer, 17th January 2018, https://www.theengineer.co.uk/magnetic-liquid-window-jena/?cmpid=tenews_4623775&utm_medium=email&utm_source=newsletter&utm_campaign=tenews&adg=25D5594B-61A5-4477-9BBF-F97F87829407)

ΕΝΔΙΑΦΕΡΟΝΤΑ - ΛΟΙΠΑ

Spectacular spans: New bridges attract visitors around the world

Bridges may be one of the oldest forms of construction, but the last few decades have seen incredible innovations, says Judith Dupré, author of the updated *Bridges: A History of the World's Most Spectacular Spans* (Black Dog & Leventhal, $29.99). Since the first edition of her book was published 20 years ago, cable-stayed bridges, which use towers to directly support a roadway, have begun to rival suspension bridges for crossing long spans, she says. In addition, bridges are getting splashier with LED lighting and striking designs. "Engineers are coming up with solutions," she says. "They are unsung heroes." She shares some new favorites with Larry Bleiberg for USA TODAY.

Penobscot Narrows Bridge and Observatory
Prospect, Maine

Engineer Linda Figg spent hours talking to midcoast Maine residents, and learned about their pride for their granite, which was used for the Washington Monument. That led her to model a 420-foot bridge tower after the D.C. obelisk, even including a viewing area at the top. It opened in 2006 as the tallest public observatory on a bridge. "It really recast the long and important history of the place," Dupré says. Observatory open seasonally.

Mike O'Callaghan–Pat Tillman Memorial Bridge
Nevada–Arizona

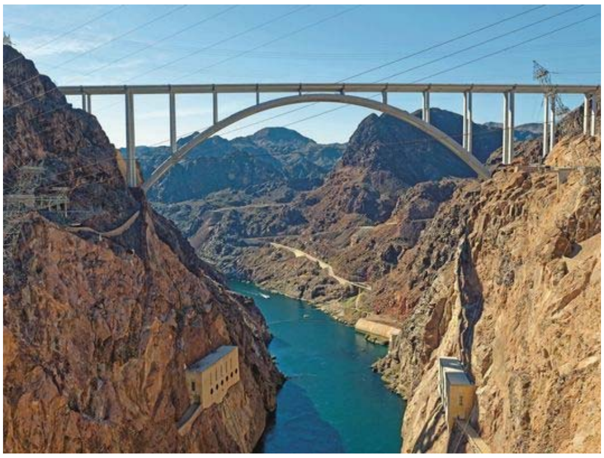

This concrete-arch Colorado River bridge opened in 2010, about 1,500-feet downstream from the Hoover Dam. It was meant to bypass the dam road, addressing traffic, security and safety concerns. "It takes its inspiration from the dam and has a structure that's really monumental," Dupré says. lvcva.com

Lucky Knot Bridge
Changsha, China

This pedestrian crossing of the Dragon King Harbor River combines several foot-bridges in a colorful red steel span that seems to dance across the water. Opened in 2016, it doesn't appear to have a beginning or end — a thrilling sequence of stairways and moon gates, Dupré says. "It's an example of creating a crossing that was needed, and designing a landmark."

Chameau Bridge
Moron, Haiti

This footbridge across Haiti's flood-prone Grand'Anse River has been a literal lifeline for villagers since opening in 2015, serving more than 40,000 people per year. It's one of hundreds of pedestrian crossings that the Denver-based nonprofit group Bridges to Prosperity has helped fund around the world. "These are being built in areas where access to a footbridge can be the difference between life and death, allowing access to markets and hospitals," Dupré says.

Laguna Garzón Bridge
Maldonado, Uruguay

Architect Rafael Viñoly combines a roundabout with a bridge to make a doughnut-shaped crossing in the middle of a coastal lagoon. It slows traffic, increases safety and has fewer support columns, a plus for marine life, Dupré says. "The cars above are moving freely, and so are the fish below."

Erasmus Bridge
Rotterdam, Netherlands

Almost completely destroyed in World War II, Rotterdam has been a laboratory of modern architecture and urban design. This light-blue steel span, completed in 1996, is a combination cable-stayed bridge, viaduct and drawbridge. It has a single asymmetrical pylon, leading to its nickname: The Swan. "It's a landmark that ties the city together," Dupré says.

Bay Bridge
San Francisco

The East Span, which opened in 2013, replaced a crossing damaged by the 1989 Loma Prieta Earthquake, and is now one of the world's widest bridges. The retrofitted West Span has a claim to fame too: It's the world's largest light art installation, illuminated by 25,000 individually programmed LEDs. "The bridge is an engineering feat, as well as an aesthetic triumph," Dupré says.

Chenab Bridge
Jammu and Kashmir, India

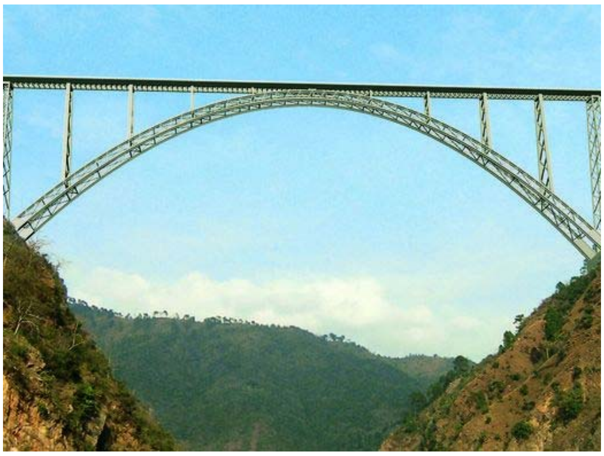

Although it won't be completed until 2020, Dupré calls this span heroic, showing the can-do spirit of workers and engineers, who are laboring in a disputed region. "It's going to be the world's tallest railway bridge, and one of the longest." Due to the remote location in northern India, supplies arrive piecemeal by truck on windy mountain roads.

Dragon Bridge
Da Nang, Vietnam

This six-lane span puts on a show, changing colors and spitting fire and water from a dragon head, making it an instant landmark when it opened in 2013. "Until the advent of LED lighting it would not have been economically feasible," Dupré says.

Zhangjiajie Glass Bridge
China

Dupré says this pedestrian bridge in a national park was built purely for fun. The glass-bottom span crosses over a gorge, nearly 1,000 feet deep. When it opened in 2016, it attracted such crowds that it had to close briefly to add facilities for visitors. "People were so eager to scare themselves to death," she says.

(Larry Bleiberg, Special for USA TODAY, Jan. 12, 2018, https://www.usatoday.com/story/travel/destinations/10greatplaces/2018/01/12/bridges-spectacular-spans-new-bridges-attract-visitors-around-world/1024818001)

Goopy GIF: You Can't Look Away from This Mesmerizing Experiment

Ferrofluid on a screw (video)

As a series of goopy platforms climb down a bolt in a mesmerizing GIF posted on Reddit, it almost looks as if Mario should hop from one to another.

But this isn't 1990's video-game graphics, it's real life. The GIF shows a demonstration of ferrofluid, a suspension of nanosize magnetic particles in oil. The magnetic particles are small and coated in a surfactant, which is a substance like soap that helps to keep the particles evenly distributed throughout the fluid, even when they're put next to a strong magnet, said Brandon Jackson, a doctoral candidate in mechanical engineering at Michigan Technological University, who has studied applications for ferrofluids.

In the GIF posted on Reddit, and in many other similar demonstrations seen on YouTube, Twitter and GIPHY, a magnet under the bolt provides the magnetic field. The liquid aligns itself with the invisible lines of the magnetic field, resulting in the spiky look. Surface tension holds the liquid together. Meanwhile, gravity pulls the liquid down the screw, resulting in the downward motion of the "platforms."

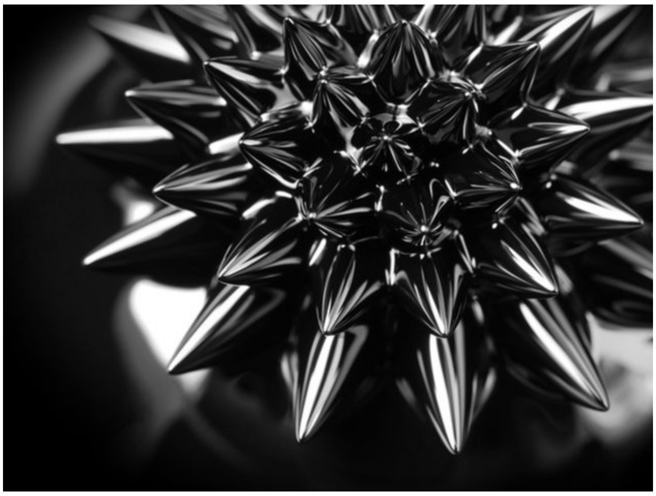

This spiky, black "thing" is actually a liquid - a ferrofluid.

The shape "is a minimum-energy solution between the gravitational energy, the surface tension energy and the magnetic energy," meaning the substance chooses the route that demands the least amount of energy, Jackson told Live Science.

In some GIFs, the demonstrator holds additional magnets, which can alter the shape of the ferrofluid further, or move it around a surface like a snuffling hedgehog.

Actually, it's rocket science

NASA scientists invented ferrofluids in the 1960s when they were trying to figure out how to efficiently move rocket fuel from a tank into an engine in a zero-gravity environment. The researchers thought that by magnetizing the fuel with tiny iron oxide particles, they might be able to use a magnetic field to suck the fuel into the engine, leaving behind any pesky gas bubbles that could cause damage, according to NASA's Technology Transfer Program.

(https://giphy.com/gifs/ferrofluid-gT9Txbff5Zznq)

Solid-rocket propellants obviated the need for the ferrofluids in space, but scientists quickly realized that ferrofluids could also be used to form seals to protect semiconductor chips during fabrication. Probably the most common industrial application today is in speakers, Jackson said. Ferrofluids are used to dampen vibrations in speaker components to prevent a distorted sound.

The future of ferrofluids

Ferrofluids make for fun science-fair demos, but they're also the subject of active research. One potential application, Jackson said, is in medicine. Some scientists have considered ferrofluids as an alternative to radiation treatment for cancer, he said. The fluids could be injected into tumors and then vibrated with a rapidly alternating magnetic field that would heat them, essentially "cooking" the tumor from the inside. Radiation similarly kills tumor cells with heat, but causes damage as it passes through tissue on the way to the cancer. Ferrofluids could similarly be used to target drugs to certain tissues, Jackson said.

Jackson and his colleagues have a different use for ferrofluids in mind. They're studying ferrofluids as self-assembling thrusters on tiny satellites. Traditional propulsion systems work well on large satellites, Jackson said, but an increasing number of the satellites shot into orbit are the size of cellphones or shoe boxes. Many use electrospray thrusters, which use tiny electrified needles to spray jets of fluid in order to propel the satellite. But the spiky hedgehog shape that ferrofluids form under the influence of a magnetic field can also shoot jets of ions — a form of propulsion that requires only a magnet, not a precision-fabricated needle.

(Stephanie Pappas / Live Science, January 13, 2018, https://www.livescience.com/61426-ferrofluid-gif.html)

Complex engineering and metal-work discovered beneath ancient Greek 'pyramid'

Latest find on Cyclades' Keros includes evidence of metal-working and suggests the beginnings of an urban centre, say archaeologists

More than 4,000 years ago builders carved out the entire surface of a naturally pyramid-shaped promontory on the Greek island of Keros. They shaped it into terraces covered with 1,000 tonnes of specially imported gleaming white stone to give it the appearance of a giant stepped pyramid rising from the Aegean: the most imposing manmade structure in all the Cyclades archipelago.

But beneath the surface of the terraces lay undiscovered feats of engineering and craftsmanship to rival the structure's impressive exterior. Archaeologists from three different countries involved in an ongoing excavation have found evidence of a complex of drainage tunnels – constructed 1,000 years before the famous indoor plumbing of the Minoan palace of Knossos on Crete – and traces of sophisticated metalworking.

The Dhaskalio promontory is a tiny island as the result of rising sea levels, but 4,500 years ago was attached by a narrow causeway to Keros, now uninhabited and a protected site. In the third millennium BC Keros was a major sanctuary where complex rituals were enacted. Earlier excavations by the team from the University of Cambridge, the Ephorate of Antiquities of Cyclades and the Cyprus Institute have uncovered thousands of marble Cycladic sculptures – the stylised human figures which inspired western artists, including Pablo Picasso – and which appear to have been deliberately broken elsewhere and brought to the island for burial.

Maintaining as well as constructing the settlement would have taken a huge communal effort. The now-deserted slopes of Dhaskalio were once covered with structures and buildings, suggesting that 4,500 years ago it was one of the most densely populated parts of the islands – despite the fact that it could not have been self-sufficient, meaning that most food, like the stone and the ore for metal working, had to be imported.

The entrance staircase from above: the sea level was much lower in the early bronze age

The first evidence of metal-working was found in excavations 10 years ago. The new finds have uncovered two workshops full of metalworking debris, and objects including a lead axe, a mould for copper daggers and dozens of ceramic fragments from metalworking equipment including the mouth of a bellows. Archaeologists will return to excavate an intact clay oven, found at the very end of the last season.

Joint director of the excavation Michael Boyd, of the University of Cambridge, said metalworking expertise was evidently concentrated at Dhaskalio at a time when access to both skills and raw materials was very limited.

A researcher holds a mould for making a spearhead from molten copper.

"What we are seeing here with the metalworking and in other ways is the beginnings of urbanisation," he said. Far-flung communities were drawn into networks centred on the site, craft and agricultural production was intensified, and the architecture became grander, gradually overshadowing the original importance of the sanctuary.

Excavated soil reveals food traces including pulses, grapes, olives, figs and almonds, and cereals, including wheat and barley. Evi Margaritis of the Cyprus Institute said: "Much of this food was imported: in the light of this evidence we need to reconsider what we know about existing networks to include food exchange."

The pyramid of terraces would have blazed in the Greek sun, visible from far off, covered in white stone imported from Naxos 10 kilometres away. The complex of drainage tunnels was discovered when archaeologists were excavating an imposing staircase in the lower terraces: research continues to discover whether they were for fresh water or sewage.

Lord Renfrew, joint director of the excavation, former Disney professor of archaeology at Cambridge and now the senior fellow at the McDonald Institute for archaeological research, first landed on Keros as a student and has returned often throughout his long career. He believes the promontory may originally have become a focus for development because it guarded the best natural harbour on the island, with wide views across the Aegean.

The excavations are being recorded digitally, using the iDig programme running on iPads for the first time in the Aegean. This creates three-dimensional models using photogrammetry recording of the entire digging process, giving everyone involved access to all data in real time.

(Maev Kennedy / The Guardian, Thu 18 Jan 2018, https://www.theguardian.com/world/2018/jan/18/complex-engineering-and-metal-work-discovered-beneath-ancient-greek-pyramid)

Engineers to mimic the human spine in construction of resilient bridge pier

A durable, low-maintenance and low-carbon bridge pier inspired by the anatomy of the human spine is being developed in the UK.

The bridge pier, which could be built in just one or two days and easily demounted at the end of its useful life, is being developed by researchers at Southampton University with funding from EPSRC. In use, it will be designed to withstand earthquakes and damage caused by traffic and cold weather.

Existing bridges, particularly those in colder countries such as the UK, US, Canada and Japan, suffer from corrosion caused by salt spreading during the winter months, meaning they require expensive maintenance, according to project leader Dr Mehdi Kashani.

"What's more, when these bridges are under dynamic loading, either from a high-speed train or an earthquake, because of the fixed way they are constructed they tend to crack, and when concrete cracks it accelerates the deterioration," said Kashani.

The human spine, in contrast, is made up of a number of vertebrae that are not fixed together, but are stacked flexibly on top of each other and so are free to move.

Between the vertebrae are intervertebral discs, which dissipate energy from the movement of the body and absorb and transmit forces without damaging the vertebrae, said Kashani.

"The vertebrae rock on top of the intervertebral discs, and the discs act as shock absorbers," he said.

The new bridge pier will be based around precast composite segments without any reinforcing steel, designed to act as the vertebrae. In between these solid segments will be "intervertebral discs", constructed from a new smart composite material being developed by the team, which will prevent the vertebrae from rubbing against each other, transfer shear forces through friction, absorb impacts caused by the rocking of the vertebrae, and provide mechanical damping under dynamic loading.

Unlike conventional composites formed of layers, which can delaminate, the new material will consist of entangled polymer fibres. Entangled materials based on titanium or metal alloys are already used in aerospace for vibration damping, said Kashani.

"We want to come up with something similar but using a polymer base," he said.

The vertebrae and discs will be tied together using a pre-tensioned un-bonded composite "tendon", designed to act like the spine's longitudinal ligament, by pulling the piers back into their central position if the bridge is subjected to lateral forces from an earthquake, for example.

(Helen Knight / the engineer, 30th January 2018, https://www.theengineer.co.uk/spine-bridge-pier/?cmpid=tenews_4693103&utm_medium=email&utm_source=newsletter&utm_campaign=tenews&adg=25D5594B-61A5-4477-9BBF-F97F87829407)

UK Researchers to Develop Composite Bridge Pier Inspired by Human Spine

Last week, the University of Southampton (UK) announced that a number of pioneering research projects at the university will be awarded funding as part of a £6.6 million investment by the Engineering and Physical Sciences Research Council (EPSRC) into the future competitiveness and creativity of the UK economy. One of those projects entails development of resilient and durable bridge pier inspired by the anatomy of the human spine.

The new bridge pier will be based around precast composite segments without any reinforcing steel designed to act as the vertebrae. In between these solid segments will be "intervertebral discs," constructed from a new "smart" composite material being developed by the team, which will prevent the vertebrae from rubbing against each other, transfer shear forces through friction, absorb impacts caused by the rocking of the vertebrae and provide mechanical damping under dynamic loading.

Everything will be tied together at the end by a composite designed to act like the spine's longitudinal ligament, which will pull the piers back into their central position if the bridge is subjected to lateral forces.

Unlike conventional composites formed of layers, which can delaminate, the new material will consist of entangled polymer fibers. Entangled materials based on titanium or metal alloys are already used in aerospace for vibration damping.

"We want to come up with something similar but using a polymer base," said Dr. Mohammad Mehdi Kashani, the leader of the project.

Kashani says that current bridges suffer from corrosion caused by salt spreading during the winter months, particularly in colder countries such as UK, US, Canada, and Japan, and therefore require expensive maintenance. They also tend to crack when exposed to dynamic loading from a high speed train or an earthquake. He believes this new bridge can be easily built in only two days and demounted at the end of its life, while the design can endure earthquakes and damage caused by traffic and cold weather.

For the next two years, the underlying science of the new spinal column will be investigated through experimental testing and numerical modeling. During the entire duration of the project, a series of review meetings, short visits to academics as well as industry partners, and an international workshop will be organized. For more information, visit http://gtr.rcuk.ac.uk.

(Evan Milberg / Composites Manufacturing, February 5, 2018, http://compositesmanufacturingmagazine.com/2018/02/uk-researchers-develop-composite-bridge-pier-inspired-human-spine)

SPINE: Resilience-Based Design of Biologically Inspired Columns for Next-Generation Accelerated Bridge Construction

Lead Research Organisation: University of Southampton, Department Name: Faculty of Engineering & the Environment

Abstract

A resilience-based design approach plays an important role in the design of new bridges and other structures. The structural elements of bridges are often directly exposed to the environment without any protection. Even though life-cycle and sustainability criteria have been incorporated in new design guidelines, there is still no design and construction technique that can fully address the future demands of a resilient and sustainable transport infrastructure.

The aim of this research is to produce innovative and transformative engineering solutions for a durable, low-maintenance, low-cost, and demountable accelerated bridge construction technique, which is resilient to environmental threats, and natural hazards. The solutions will include a completely new resilience-based bridge design approach and biologically inspired composite columns for next-generation accelerated bridge construction.

Towards this goal, this research will construct an innovative composite bridge column, which is inspired by the mechanics of the human spine. In the human spine, intervertebral discs provide flexibility, dissipate energy from the movements of the human body, and absorb and transmit forces without damaging the vertebrae bones. The proposed spinal bridge column will be constructed using precast composite segments (the 'vertebrae'). A new smart composite material will be developed and used in between of these solid composite segments (the 'intervertebral discs'). This will keep the vertebrae from rubbing against each other, transfer the shear forces through friction, absorb the impact due to the rocking of vertebrae, and provide mechanical damping under dynamic loading. Finally, the vertebrae and intervertebral discs will be tied together using an unbonded composite post-tensioning tendon (the 'longitudinal ligament'), to provide self-centring mechanism in the column when subjected to lateral force.

In this 24 moths research, the underlying science of the new spinal column will be investigated through experimental testing and numerical modelling. During the entire duration of the project a series of review meetings, short visits to academics as well as industry partners, and an international workshop will be organised. This interaction is deemed vital for the co-development of new concepts, the transfer of know-how and the resilient and sustainable accelerated bridge construction.

Planned Impact

Transport infrastructure has a significant impact on the quality of people's everyday life. The new resilience-based bridge design, spinal columns, and accelerated bridge construction technique that will be developed in this research, will provide a means to the next generation of resilient and sustainable transport infrastructure (the key impact). This is a major requirement as our national transport infrastructure approaches the end of its design life and does not meet the future demands. Therefore, we urgently need to upgrade our transport infrastructure, and adapt it to future demands as well as environmental impacts due to climate change. More specifically the expected impacts of this research will include:

Contributing to UK economy and society: The outcomes of this research will help civil engineering industry by developing innovative spinal composite bridge columns for next-generation accelerated bridge construction, which is also resilient to environmental threats and natural hazards. This can be directly used in construction of new bridges and replacing ageing, and often structurally deficient, bridges that are approaching or already reached the end of their service life. This will help reducing the direct and indirect construction cost, reducing the maintenance cost of the new bridges, and make the transport infrastructure resilient and sustainable. As a result, downtime in infrastructure networks will be minimised, the safety will be improved, and tax payers' money will be saved.

Strengthening UK competitiveness: This programme will also strengthen the UK's civil/structural engineering sector. This is important in the face of the fierce global competition and the current economic climate. The outcomes of this research will provide the UK engineers with novel solutions and tools for design and construction of structures around the world in a time-efficient manner. The new resilience-based bridge design, the innovative spinal columns, and the new accelerated bridge construction technique will have a large international market, with the UK engineers taking a lead to the benefit of UK plc.

Ensuring UK leadership in engineering: The dissemination activities that will accompany this research programme (see Pathways to Impact) will ensure the international visibility of UK academia. This will maintain and increase the UK's leading position in engineering and will indirectly generate business for UK entities (companies, industries, consultancy firms, etc.).

Creating new skills: To ensure a rapid transition from leading edge research to practical deployment, I will work closely with my industry partners. This will have a significant impact in forging closer links with industry leading to support for my PDRA and PhD students, and help to establish my team as a global centre of excellence in resilience-based design of transport infrastructure. In addition, it has the potential that a series of companies and bridge owners (e.g. Network Rail and Highways England) to adopt my approach, and act as promoter to the wider community.

More
The World's Most Spectacular Bridges

As a child growing up on the Eastern Shore of Maryland, crossing a big bridge meant entering a portal to a new world. The majestic, dual-span Chesapeake Bay Bridge and the 23-mile-long Chesapeake Bay Bridge Tunnel were our two main routes off of the rural shore towards "real cities" and airports with more than two gates. But they were also a trip in themselves— a chance to spot bottlenose dolphins and peregrine falcons, a chance to see both our home, and our destination, from a new, brave perspective.

Bridges all around the world, from West Virginia's New River Gorge, to Dublin's Samuel Beckett, to Myanmar's U Bein, serve this same purpose, giving every type of traveler an opportunity to connect and explore. Whether you're the glass-bottom-bridge-thrill-seeker type, or a Francophile drifting south from Paris, we've got a bridge for you.

Here are 12 bridges we just can't get over.

IF YOU'RE IN FOR A LITTLE MISCHIEF…
Die Rakotzbrücke: Kromlau Park, Kromlau, Germany (Rakotzbrücke Bridge)

Commissioned by Friedrich Hermann Rötschke in 1860, Rakotzbrücke's perfect parabola and basalt spires make it a legendary "devil's bridge." According to Rakotz-brücke's myth, the builder crossed the finished bridge, sacrificing himself in exchange for the devil's help. Board the Muskau Forest Railway to visit during spring rhododendron bloom.

You can also visit other devil's bridges in Switzerland, Bulgaria, Italy, Wales, France, England, Spain and Arizona.

IF YOU'RE A NATURE LOVER…
Living Root Bridge: Nongriat, India

The name gives it all away: The Living Root Bridge is made from living, grounded tree roots so that it is not washed away by floods.

Nongriat, India is one of the world's wettest places—a jungle of waterfalls, beehives, and betel nut trees. For hundreds of years local Khasi have dealt with seasonal river surges by weaving living footbridges out of Indian rubber tree roots. Umshiang, a double-decker (soon to be triple-decker) root bridge is expected to survive several hundred years and can support the weight of 50 people at once.

For even more fresh air (both in and out of the city) visit Langkawi Sky Bridge, or Natural Bridges in Virginia, Alabama, Arkansas, or Seoul Skygarden.

IF PHYSICS IS YOUR FAVORITE SUBJECT…
Rolling Bridge: London, England

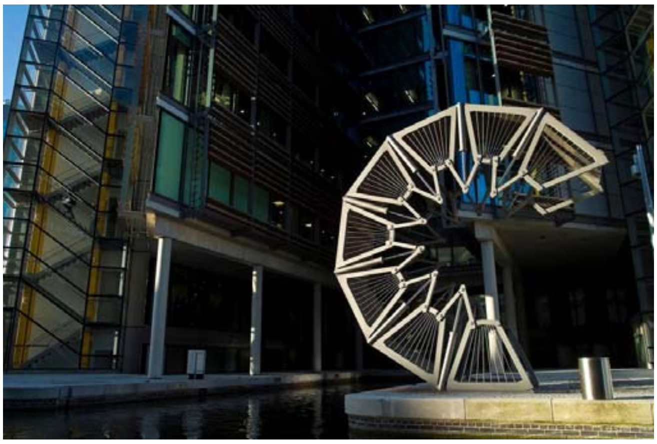

Completed in 2004, Heatherwick Studio's Rolling Bridge provides access to the Grand Union Canal in London's Paddington Basin. The bridge's eerily quiet hydraulics were inspired by Stan Winston's animatronic dinosaur tails from the film *Jurassic Park*. The shiny steel beams of nearby Paddington Fan Bridge mimic a Japanese fan as they cantilever open to boat traffic every Wednesday and Friday at noon.

To see other unexpected designs, visit Netherland's Moses Bridge, Beijing's Lucky Knot Bridge, and the infamous "Blinking Eye."

IF YOU'RE NOT AFRAID OF HEIGHTS...
Inca Rope Bridge: Akpurimac River, Peru

Each year the Q'eswachaka is untied and woven a new by local bridge builders.

Q'eswachaka, one of the last surviving Inca rope bridges, has spanned 124 feet across the Akpurimac canyon for more than 500 years. Every June, local bridge builders, Eleuterio Callo Tapia, Victoriana Arizapana, and their neighbors, gather to untie the existing bridge and weave a new one out of local *ishu* grass. The ancient bridge-building ritual is then celebrated with traditional song and dance.

Jet-setting north of the equator? Spot puffins and sharks from Ireland's 100-foot-high Carrick-a-Rede Rope Bridge—first constructed by salmon fishermen in 1755. And if that's not high enough, take a drive across France's Millau Viaduct or China's record-setting Beipanjiang Bridge—a whopping 1,854 feet above the Beipan River.

IF YOU'RE ON TWO WHEELS...
Webb Bridge: Docklands, Melbourne, Australia

The Webb Bridge connects the Docklands to Victoria Harbor in Melbourne, Australia.

The Guditjmara people have been harvesting eels in Lake Condah, Victoria, for more than 6,000 years, using a system of canals and traps that is one of the earliest surviving examples of freshwater aquaculture. These basket-woven Koori eel traps served as inspiration for Melbourne's Webb Bridge, designed by world-renowned sculptor Robert Owen. Webb Bridge is best explored by bike via the Capital City Trail or by paddling the Yarra River on a moonlight kayak tour.

Other bike-friendly bridges include Copenhagen's Bicycle Snake, The Big Dam Bridge in North Little Rock, Arkansas, Portland's Tilikum Crossing, and Sweden's Sölvesborg.

IF YOU LIKE LONG WALKS IN THE SKY...
Charles Kuonen Suspension Bridge: Zermatt, Switzerland

At 1,620 feet long, the Charles Kuonen Suspension Bridge in Zermatt is the longest suspension footbridge in the world. Fairytale-worthy views of the Matterhorn may just be enough to distract you from the 278-foot drop between you and the valley floor.

Other sky-high bridges to walk if you dare: China's new Hongyagu Glass-Bottom Bridge, Highline 179, Grandfather Mountain's Mile High Swinging Bridge, and Austria's Dachstein Glacier suspension bridge to the glass-walled Stairway of Nothingness.

IF YOU'RE A ROMANTIC...
Bridge of Sighs: Rio di Palazzo, Venice, Italy

Poets, painters, and opera singers have swooned over Ponte dei Sispori, Venice's Bridge of Sighs, for centuries. And gondoliers claim that kissing below the bridge during sunset, as the bells of St. Mark's toll, is a surefire recipe for everlasting love. The connecting palace offers tours through the bridge with blue-lagoon views of San Giorgio Maggiore. Kayak the Rio di Palazzo beneath the bridge to see its 17^{th}-century limestone *mascarons*, ornately carved masks meant to ward off evil spirits.

Other starry-eyed bridge strolls: the Si-o-se-pol Bridge in Iran, the Yeojwacheon Romance Bridge in South Korea, and the geranium-flooded 17th-century frescoes of Kapellbrücke in Lucerne, Switzerland.

IF YOU LOVE A LITTLE "SUSPENSE"...
Golden Gate Bridge: San Francisco

Over three million vehicles cross San Francisco's Golden Gate Bridge every month. Skip the bus-fumy bridge sidewalk and opt for a bird's-eye view of the mountain-high suspension bridge from Hawk Hill's new trail, complete with easier slopes, new signage, and new guard rails. Or whale watch while lounging on a deck trampoline as you sail beneath the bridge at sunset.

Other epic suspension bridges include Japan's Akashi Kaikyo Bridge, Tower Bridge, Brooklyn Bridge, and Colorado's Royal Gorge.

IF YOU LIKE TO LINGER...
Henderson Waves Bridge: Singapore

The Henderson Waves Bridge in Singapore is great for bird watching at sunrise, or from 7 p.m. to 2 a.m. each evening when LED lights make it shine.

Steel and local Balau wood curve together to form the spectacular Henderson Waves, the highest pedestrian bridge in Singapore. The bridge connects Telok Blangah Hill Park and Mount Faber Park as a part of the six-mile-long Southern Ridges walk. Visit the bridge at sunrise for less crowds and excellent birdwatching, including a chance to see the rare black baza.

Other treetop bridges worth a linger: Vancouver's Capilano Suspension Bridge, the Kirstenbosch Boomslang Tree Canopy, Baumwipfelpfad in Germany, and the Inkaterra Canopy.

IF YOU'RE IN FOR AN ADVENTURE...
Pont du Gard: Vers-Pont-du-Gard, France

Arching over the Gardon River halfway between Nîmes and Uzès sits the massive Pont du Gard, a limestone aqueduct built by the Romans roughly 2,000 years ago. Visit in summer for a leisurely paddle and afternoon swim, then wind your way past a 1,000-year-old olive tree on the way to Les Terraces for a sunset glass of Clairette.

Want more than a calm kayak? Visit Bosnia's Stari Most for diving, Sydney Harbor Bridge for climbing, and Skypark Sochi for skybridge walks and bungee-jumping.

IF YOU'RE A HISTORY BUFF...
Edmund Winston Pettus Bridge: Selma, Alabama

President Barack Obama, First Lady Michelle Obama, and the First Family are joined by former President George W. Bush, former First Lady Laura Bush, Rep. John Lewis, D-Ga., former foot soldiers and other dignitaries to march across the historic Edmund Pettus Bridge in 2015.

On March 7, 1965, 600 voting rights activists, led by Dr. Martin Luther King Jr., began marching across Selma's Edmund Pettus Bridge towards Montgomery, Alabama. Due to the bridge's design, they couldn't see the violent counter-protestors waiting for them on the other side. And when that obstacle did appear, they marched forward anyway. Two weeks later, the march began again, successfully, with not 600, but more than 3,000 marchers. The annual Selma Bridge Crossing Jubilee honors this historic moment of bravely moving forward even when the end is unknown.

Other bridges that have made their mark on history are: Turkey's Taşköprü, West Virginia's Philippi Covered Bridge, Israel's Ad Halom, and Spain's Alcántara.

IF YOU LIKE TO UP YOUR STEPS ON VACATION…
Stepping stone bridge: Fenghuang, China

A traditional *dingbu* bridge, made of cut and sunken stones, stretches across the Tuojiang River in China's Phoenix Ancient Town. Further up the river sits the Ming-dynasty Hongqiao, a lantern-strung, three-arch stone pavilion bridge. Its second-level teahouse offers comfy rattan chairs and unbeatable river views of *diaojiaolou* stilt houses, dragon boat racing, and, sometimes, some rather startled ducks.

Wander down other lovely footbridges in London, Paris, Bilbao, Spain, and Flims, Switzerland.

This list was compiled with the help of structural and civil engineers, Mark R. Cruvellier and Stephen Ressler. Cait Etherton is a Virginia-based writer and frequent contributor to National Geographic Travel. *Follow her journey on Twitter.*

(Caitlin Etherton / National Geographic Travel, January 31, 2018, https://www.nationalgeographic.com/travel/lists/activities/best-bridges-in-world/?utm_source=NGdotcom-Travel&utm_medium=Email&utm_content=20180208_Travel_Newsletter&utm_campaign=NGdotcom&utm_rd=1084349954)

ΝΕΕΣ ΕΚΔΟΣΕΙΣ ΣΤΙΣ ΓΕΩΤΕΧΝΙΚΕΣ ΕΠΙΣΤΗΜΕΣ

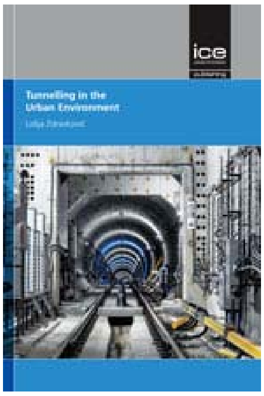

Tunnelling in the Urban Environment (Géotechnique Symposium in Print 2017)

Edited by Lidija Zdravkovic

With urban tunnel construction growing worldwide, the ability to accurately predict the ground and structural response to tunnelling and the associated risks is now more important than ever before. Engineers are expected to consider all aspects of tunnel engineering in order to safeguard existing infrastructure, by employing field monitoring, physical modelling and numerical analysis in developing a detailed knowledge of multiple soil–structure interactions.

The *Géotechnique Symposium in Print* took place at the Institution of Civil Engineers on 14th September 2017 to discuss the wider aspects of tunnelling in urban locales. The papers included here bring together important international research presented at the symposium and featured in Géotechnique. Topics of discussion, amongst others, included:

- case studies from Crossrail, CTRL and Barcelona metro projects
- open-face tunnelling effects on non-displacement piles in clay
- influence of building characteristics on tunnelling-induced ground movements
- impact of new tunnel construction on structural performance of existing tunnels.

Tunnelling in the Urban Environment offers practitioners and researchers alike with important coverage of the increasingly complex and varied challenges engineers have to face when constructing tunnels in urban centres.

(ICE Publishing, 24/01/2018)

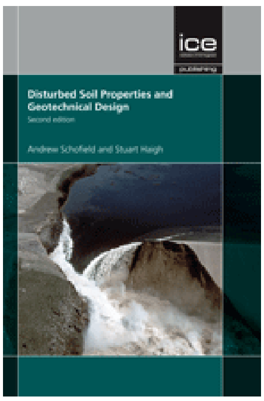

Disturbed Soil Properties and Geotechnical Design, Second Edition

Andrew Schofield and Stuart Haigh

Disturbed Soil Properties and Geotechnical Design, Second edition describes the developments leading to the Original Cam Clay model, focusing on fundamentals of the shearing of soil. The first edition explained and illustrated fallacies in past work of engineering geologists, and laid groundwork for the understanding that should form the basis of modern geotechnical design.

With the changing environment, and the increasing size of construction projects, engineers now need a better understanding of ground behaviour to prevent future catastrophes such as the 1976 Teton Dam failure shown on the cover. The further additions in this book will help geotechnical engineers acquire this knowledge.

Disturbed Soil Properties and Geotechnical Design, Second edition:

- provides an outline of the energy-based Cam-clay approach that can predict geotechnical deformations
- illustrates further fallacies in commonly used c-φ Coulomb soil mechanics
- describes the use of centrifuge modelling in geotechnical design, based on examples from the last four decades

Once armed with the simple concepts of wet/weepy and dry/thirsty sides of the critical state line, readers will better understand if soil will tend to contract or dilate in drained shearing, and if pore pressures caused by undrained shearing will be positive or negative

Full of technical and personal insights, this is a rewarding book that forces the rethinking of modern geotechnical engineering. Much like the first edition, this book remains an invitation for the unconverted to re-examine the basic understanding of soil behaviour, and for the converted to ensure that the teaching, vocabulary and nomenclature used in describing strength models for soil, accurately reflect the underlying concepts.

(ICE Publishing, 22/11/2017)

ΗΛΕΚΤΡΟΝΙΚΑ ΠΕΡΙΟΔΙΚΑ

www.geoengineer.org

Κυκλοφόρησε το Τεύχος #152 του **Newsletter** του **Geoengineer.org** (Ιανουαρίου 2018) με πολλές χρήσιμες πληροφορίες για όλα τα θέματα της γεωμηχανικής. Υπενθυμίζεται ότι το Newsletter εκδίδεται από τον συνάδελφο και μέλος της ΕΕΕΕΓΜ Δημήτρη Ζέκκο (secretariat@geoengineer.org).

Ενδεικτικά αναφέρονται:

- At least 26 killed in Philippines by landslides caused by tropical storm (video)
- 5 dead, 15 missing after mudslide in southern Chile (video)
- Watch the unique video with a selection of the most captivating news that were posted in its Geotechnical News Center in 2017
- Scientists to map areas at risk from liquefactio (video)
- Freetown's landslide and flooding disaster was 90 percent man-made
- Strong earthquake hits southeastern Iran, no casualties reported
- Fifty simulations show how a magnitude 9.0 Cascadia earthquake could play out
- Gravity signals could rapidly quantify the magnitude of strong earthquakes

http://campaign.r20.constantcontact.com/render?m=1101304736672&ca=7697aa45-cad8-41a7-a136-059c036a05ff

ΕΚΤΕΛΕΣΤΙΚΗ ΕΠΙΤΡΟΠΗ ΕΕΕΕΓΜ (2015 – 2018)

ΕΕΕΕΓΜ

Τομέας Γεωτεχνικής
ΣΧΟΛΗ ΠΟΛΙΤΙΚΩΝ ΜΗΧΑΝΙΚΩΝ
ΕΘΝΙΚΟΥ ΜΕΤΣΟΒΙΟΥ ΠΟΛΥΤΕΧΝΕΙΟΥ
Πολυτεχνειούπολη Ζωγράφου
15780 ΖΩΓΡΑΦΟΥ

Τηλ. 210.7723434
Τοτ. 210.7723428
Ηλ-Δι. secretariat@hssmge.gr ,
geotech@central.ntua.gr
Ιστοσελίδα www.hssmge.org (υπό κατασκευή)

«ΤΑ ΝΕΑ ΤΗΣ ΕΕΕΕΓΜ» Εκδότης: Χρήστος Τσατσανίφος, τηλ. 210.6929484, τοτ. 210.6928137, ηλ-δι. ctsatsanifos@pangaea.gr, editor@hssmge.gr, info@pangaea.gr

«ΤΑ ΝΕΑ ΤΗΣ ΕΕΕΕΓΜ» «αναρτώνται» και στην ιστοσελίδα www.hssmge.gr